

Comparative apicomplexan cell division

Fussing about fission: defining variety among mainstream and exotic apicomplexan cell division modes

Marc-Jan Gubbels^{1§}, Caroline D. Keroack², Sriveny Dangoudoubiyam^{3*}, Hanna L. Worliczek^{1,4,#}, Aditya S. Paul², Ciara Bauwens¹, Brendan Elsworth^{2,5}, Klemens Engelberg¹, Daniel K. Howe³, Isabelle Coppens⁶, Manoj T. Duraisingh^{2§}

¹ Department of Biology, Boston College, Chestnut Hill, MA

² Department of Immunology and Infectious Diseases, Harvard T. H. Chan School of Public Health, Harvard University, Boston, MA

³ Gluck Equine Research Center, Department of Veterinary Science, University of Kentucky, Lexington, KY

⁴ Institute of Parasitology, University of Veterinary Medicine, Vienna, Austria

⁵ School of Biosciences, University of Melbourne, Melbourne, Australia

⁶ Department of Molecular Microbiology and Immunology, Bloomberg School of Public Health, Johns Hopkins University, Baltimore, MD

§ Correspondence:

Marc-Jan Gubbels

gubbelsj@bc.edu

Manoj T. Duraisingh

mduraisi@hsph.harvard.edu

*present address: Department of Comparative Pathobiology, Purdue University College of Veterinary Medicine, West Lafayette, IN

#present address: Department of History, University of Vienna, Vienna, Austria

Comparative apicomplexan cell division

29 **Keywords:** Apicomplexa, cell division, cell cycle, karyokinesis, schizogony, endodyogeny,
30 endopolygeny, binary fission

31

32 **Abstract**

33 Cellular reproduction defines life, yet our textbook-level understanding of cell division is limited
34 to a small number of model organisms centered around humans. The horizon on cell division
35 variants is expanded here by advancing insights on the fascinating cell division modes found in
36 the Apicomplexa, a key group of protozoan parasites. The Apicomplexa display remarkable
37 variation in offspring number, whether karyokinesis follows each S/M-phase or not, and whether
38 daughter cells bud in the cytoplasm or bud from the cortex. We find that the terminology used to
39 describe the various manifestations of asexual apicomplexan cell division emphasizes either the
40 number of offspring or site of budding, which are not directly comparable features and has led to
41 confusion in the literature. Division modes have been primarily studied in two human pathogenic
42 Apicomplexa, malaria-causing *Plasmodium* spp. and *Toxoplasma gondii*, a major cause of
43 opportunistic infections. *Plasmodium* spp. divide asexually by schizogony, producing multiple
44 daughters per division round through a cortical budding process, though at several life-cycle
45 nuclear amplifications are not followed by karyokinesis. *T. gondii* divides by endodyogeny
46 producing two internally budding daughters per division round. Here we add to this diversity in
47 replication mechanisms by considering the cattle parasite *Babesia bigemina* and the pig parasite
48 *Cystoisospora suis*. *B. bigemina* produces two daughters per division round by a ‘binary fission’
49 mechanism whereas *C. suis* produces daughters through both endodyogeny and multiple internal
50 budding known as endopolygeny. In addition, we provide new data from the causative agent of
51 equine protozoal myeloencephalitis (EPM), *Sarcocystis neurona*, which also undergoes
52 endopolygeny but differs from *C. suis* by maintaining a single multiploid nucleus. Overall, we
53 operationally define two principally different division modes: internal budding found in cyst-
54 forming Coccidia (comprising endodyogeny and two forms of endopolygeny) and external
55 budding found in the other parasites studied (comprising the two forms of schizogony, binary
56 fission and multiple fission). Progressive insights into the principles defining the molecular and
57 cellular requirements for internal versus external budding, as well as variations encountered in
58 sexual stages are discussed. The evolutionary pressures and mechanisms underlying
59 apicomplexan cell division diversification carries relevance across Eukaryota.

Comparative apicomplexan cell division

60 **Contribution to the Field**

61
62 Mechanisms of cell division vary dramatically across the Tree of Life, but the mechanistic basis
63 has only been mapped for several model organisms. Here we present cell division strategies
64 across Apicomplexa, a group of obligate intracellular parasites with significant impact on
65 humans and domesticated animals. Asexual apicomplexan cell division is organized around
66 assembly of daughter buds, but division forms differ in the cellular site of budding, number of
67 offspring per division round, whether each S-phase follows karyokinesis and if mitotic rounds
68 progress synchronously. This varies not just between parasites, but also between different life-
69 cycle stages of a given species. We discuss the historical context of terminology describing
70 division modes, which has led to confusion on how different modes relate to each other.
71 Innovations in cell culture and genetics together with light microscopy advances have opened up
72 cell biological studies that can shed light on this puzzle. We present new data for three division
73 modes barely studied before. Together with existing data, we show how division modes are
74 organized along phylogenetic lines and differentiate along external and internal budding
75 mechanisms. We also discuss new insights into how the variations in division mode are regulated
76 at the molecular level, and possess unique cell biological requirements.

Comparative apicomplexan cell division

77 1 Introduction

78 Reproduction is critical for perpetuating a species and lies at the core of the definition of life.
79 Yet, the modes by which cell division can occur are very diverse. The molecular and cellular
80 mechanisms underlying such differences have been dissected for a limited set of model
81 organisms, most of which carry resemblance to mammalian/human cell division. The
82 Apicomplexa comprise a protozoan phylum harboring human pathogens, like malaria-causing
83 *Plasmodium* spp., opportunistic parasites like *Toxoplasma gondii* and *Cryptosporidium* spp., and
84 emerging pathogens like *Babesia* spp. (phylogeny in Fig 1). In addition, many are of economic
85 relevance in agriculture and companion animals such as *Babesia* spp, *Theileria* spp. and *Eimeria*
86 spp. Furthermore, many Apicomplexa infect other birds, mammals, reptiles, amphibians, fish,
87 and invertebrates, but their cell biology has only been studied minimally. The asexual
88 multiplication cycles of the Apicomplexans are diverse, and their sexual cycles add even more
89 diversity. The well-studied Apicomplexa relevant to humans display a diverse spectrum of
90 asexual cell division strategies both within and among species, providing an excellent
91 opportunity for comparative biology. Indeed, we posit that by studying the principles in more
92 distant organisms such as protozoa, which span a wide breadth of evolutionary history and
93 correspondingly diverse biology, we can obtain fascinating new insights and principles.

94 Asexual apicomplexan cell division revolves around variations in budding through the
95 assembly of a membrane skeleton that ultimately underlies the plasma membrane. The
96 beginning- and end-point of a cell division round across all Apicomplexa is a “zoite”, a cell type
97 with the phylum-defining complex of apical secretory organelles and cytoskeletal structures
98 (Leander and Keeling, 2003) (e.g. Fig 2A, 3F1, 4A, 5E1, 6C1). These apical structures uniformly
99 facilitate host-cell invasion, an essential step in the obligate intracellular life style of
100 apicomplexan parasites (Gubbels and Duraisingh, 2012; Sharma and Chitnis, 2013; Frenal et al.,
101 2017a). The cortical cytoskeleton just below the plasma membrane, however, plays an additional
102 role as a key structure facilitating budding across asexual division modes for Apicomplexa
103 (Anderson-White et al., 2012; Kono et al., 2016). From the outside in, it is built up from three
104 uniformly conserved elements: alveolar vesicles (alveoli) that anchor the myosin motor enabling
105 motility (Frenal et al., 2017a), an epiplastin (a.k.a. alveolar) protein meshwork (Goodenough et
106 al., 2018), and a series of sub-pellicular, longitudinal microtubules emanating from the apical
107 end. The number and length of the microtubules vary across parasite species and stage (Spreng et

Comparative apicomplexan cell division

108 al., 2019), but the alveoli and epiplastin meshwork are universally conserved and make up the
109 inner membrane complex (IMC) (Kono et al., 2012). The epiplastin family proteins contain Val-
110 Pro-Val (VPV) repeats and are generally known as alveolins or IMC proteins (Gould et al., 2008;
111 Anderson-White et al., 2011; Kono et al., 2012; Al-Khattaf et al., 2015). Cytoskeletal assembly
112 initiates from the centrosome and all three elements are simultaneously assembled in an apical to
113 basal direction (Chen and Gubbels, 2013; Francia and Striepen, 2014; Suvorova et al., 2015).
114 Another important and shared feature is that across asexual division modes, budding appears to
115 be tied always to a round of S-phase and mitosis (Francia and Striepen, 2014; Suvorova et al.,
116 2015). A fourth cytoskeleton element that is conserved across division modes is the basal
117 complex, a ring residing at the basal end of the daughter bud (Ferguson et al., 2008). This ring
118 contains MORN1, a scaffolding protein that is essential for maintenance of the daughter bud's
119 basal end integrity (Gubbels et al., 2006; Hu, 2008; Heaslip et al., 2010; Lorestani et al., 2010;
120 Kono et al., 2016). Proteins with repetitive MORN domains are often found in cilia and flagella
121 (Mecklenburg, 2007; Shetty et al., 2007; Tokuhiko et al., 2008; Morriswood and Schmidt, 2015);
122 indeed all apicomplexan division modes share several features with cilia or flagella assembly as
123 seen across eukaryotes. For example, striated fiber assembly (SFA) fibers are found in flagellar
124 assembly in algae to orient the basal body in the flagellum, which in Apicomplexa anchor the
125 centrosome in the daughter bud (Francia et al., 2012). A spindle assembly abnormal protein 6
126 (SAS6)-like protein found in flagellar basal bodies is also found in the apical polar ring (APR),
127 the microtubule organizing center (MTOC) nucleating the subpellicular microtubules (and
128 conoid, if present) (de Leon et al., 2013; Francia et al., 2015; Wall et al., 2016). Finally, the base
129 of cilia and flagella is often decorated with a contractile centrin and a myosin (Roberts et al.,
130 2004; Trojan et al., 2008), which, at least in *T. gondii*, are represented by TgCentrin2 and
131 Myosin I and J (Hu et al., 2006; Hu, 2008; Frenal et al., 2017b).

132 Despite this central plan, many variations exist on what precedes daughter budding, and how
133 daughter bud formation is orchestrated. The first variable is the number of offspring per mother
134 cell in an asexual apicomplexan division round, which can be as few as two or nearly 100,000.
135 The principle behind the uncoupling of daughter formation from S/M-phase was recently
136 established in *T. gondii* by the presence of a bipartite centrosome: the centrosome's inner-core
137 proximal to the nucleus regulates the S/M cycle independently of the centrosome's outer-core
138 distal from the nucleus, which organizes daughter bud formation (Chen and Gubbels, 2013;

Comparative apicomplexan cell division

139 Suvorova et al., 2015; Chen and Gubbels, 2019). Moreover, cyclins and cyclin-dependent
140 kinases (CDKs), as found in higher eukaryotes, ultimately control cell cycle progression but their
141 nature and modes of operation are specifically tailored to the needs of different apicomplexan
142 cell cycle variation (e.g. (Roques et al., 2015; Alvarez and Suvorova, 2017; Ganter et al., 2017;
143 Naumov et al., 2017), recently reviewed in (Matthews et al., 2018; White and Suvorova, 2018)).
144 A second variable is whether karyokinesis follows each S-phase and mitosis (S/M-phase) or not.
145 Finally, daughters can either assemble within the mother's cytoplasm (internal budding), or
146 assemble and emerge directly from the plasma membrane of the mother cell (cortical or
147 peripheral budding). Strikingly, these modes can vary not only between Apicomplexa, but also
148 across different life-cycle stages within a single species.

149 Although these insights describe the key principles, the details on cell biological mechanisms
150 facilitating the various division modes are intermittent and often compounded by historical
151 terminology which either do not accurately capture the shared principles or clearly define
152 differences. Here we highlight the best-understood cell division modes, schizogony in
153 *Plasmodium* spp. and endodyogeny in *T. gondii*, supplemented with new data on emerging
154 systems displaying different forms of endopolygeny in *Cystoisopora suis* and *Sarcocystis*
155 *neurona*, as well as binary fission in *Babesia bigemina*. Emerging insights are subsequently used
156 to assess their kinship and to chart principles underlying these distinct cell division modes.

157

158 **2 Material and Methods**

159 **2.1 Babesia spp. culture**

160 *B. bigemina* strain JG-29 (Mexico) was kindly provided by Dr. David Allred (University of
161 Florida) and grown as described previously (Vega et al., 1985) with modifications as described
162 here. Parasites were culture adapted over a month to grow efficiently in tissue culture media
163 RPMI-1640 supplemented with 25 mM HEPES, 50 mg/l hypoxanthine, 2.42 mM sodium
164 bicarbonate, and 4.31 mg/ml AlbuMAX-II (Invitrogen). Before addition of AlbuMAX-II and
165 sodium bicarbonate, the pH was adjusted to 6.75. Parasites were grown under microaerophilous
166 stationary phase culture conditions with a hypoxic atmosphere of 1:5:94 oxygen: carbon dioxide:
167 nitrogen at 4% hematocrit in washed, defibrinated bovine red blood cells (Hemostat Labs, Dixon,
168 CA).

Comparative apicomplexan cell division

169 *B. divergens* strain Rouen 1987, a kind gift from Drs. Kirk Deitsch and Laura Kirkman
170 (Weill Cornell Medical College), was grown in human erythrocytes as described (Paul et al.,
171 2016). Human erythrocytes were purchased from Research Blood Components (Boston, USA).

172

173 **2.2 *Cystoisospora suis* culture**

174 Oocysts of *C. suis* strain Wien-I (Austria) were isolated from porcine fecal samples and used for
175 *in vitro* culture in intestinal porcine epithelial cells (IPEC-J2, ACC 701, Leibniz Institute DSMZ
176 GmbH, Braunschweig, Germany) as described previously (Worliczek et al., 2013) with
177 modifications as described here. For the production of glass cover slips with confluent layers of
178 host cells infected with *C. suis*, cover slips were placed into 6-well culture plates for suspension
179 cultures (PAA, Pasching, Austria). IPEC-J2 were suspended in DMEM/Ham's F12 medium
180 (PAA, Austria) supplemented with 5 % fetal calf serum, 2 mM L-glutamine, 100 U/ml penicillin
181 and 0.1 mg/ml streptomycin, and seeded in a density of 4×10^5 cells/well. After overnight
182 incubation at 37°C, 5 % CO₂ cover slips with attached IPEC-J2 were transferred to 6-well
183 surface-treated culture plates for adherent cells (PAA, Austria). Sporozoites of *C. suis* were
184 excysted as described previously (Worliczek et al., 2013), suspended in culture medium and
185 applied to the host cells in a density of sporozoites:host cells of 1:30. The infected cell cultures
186 were incubated at 37°C, 5% CO₂ and culture medium was exchanged at 1, 4, and 7 days post
187 infection (dpi).

188

189 **2.3 *S. neurona* culture and immunofluorescence assays**

190 *S. neurona* strain SN3 was cultured, transfected and processed for immunofluorescence as
191 described before (Dubey et al., 2017; Howe et al., 2018). In short, parasites were cultured and
192 maintained in bovine turbinate (BT) cell monolayers. For IFA, extracellular merozoites were
193 used to infect BT cells in 24-well plates containing coverslips. Typically, on day 3 post infection,
194 infected BT cell monolayers were methanol-fixed for downstream immunofluorescence
195 experiments. Freshly isolated extracellular *S. neurona* merozoites were used for transient
196 expression of YFP-tagged TgIMC15 (Anderson-White et al., 2011).

197

198 **2.4 *B. bigemina* immunofluorescence assays**

Comparative apicomplexan cell division

199 *B. bigemina* indirect immunofluorescence assays were performed on >10% parasitemia bovine
200 red blood cells by air drying drops in 10-well slides (Electron Microscopy Sciences), followed
201 by 100% methanol fixation for 5 min at -20°C, 3 rinses in PBS and blocking in 3% BSA in PBS
202 for 1 hr at RT. Primary antibodies diluted in blocking solution (rabbit TgCentrin1 1:4000 (Fung
203 et al., 2012), mouse MAb 12G10 α -tubulin 1:100 (University of Iowa Hybridoma Bank) (Jerka-
204 Dziadosz et al., 1995); mouse ascites MAb B-5-1-2 α -tubulin 1:200 (Sigma-Aldrich #T5168); rat
205 TgEB1 1:100 (Chen and Gubbels, 2019); guinea pig BbIMC1a 1:500) were incubated for 1 hr at
206 RT, followed by 3 washes for 5 min in PBS, Alexa488 or 594 conjugated secondary antisera
207 (ThermoFisher) diluted 1:400 in 0.1% BSA in PBS for 45 min at RT followed by 1 wash for 5
208 min in PBS containing 1.5 μ g/ml 4',6-diamidino-2-phenylindole (DAPI) to stain DNA, and two
209 additional 5 min washes with PBS before mounting with Fluoro-Gel (Electron Microscopy
210 Sciences). A Zeiss Axiovert 200 M wide-field fluorescence microscope was used to collect
211 images, which were deconvolved and adjusted for phase contrast using Volocity software
212 (Quorum Technologies). SR-SIM was performed on a Zeiss ELYRA S.1 system in the Boston
213 College Imaging Core in consultation with Bret Judson. All images were acquired, analyzed and
214 adjusted using ZEN software and standard settings.

215

216 **2.5 *C. suis* indirect immunofluorescence assays**

217 *C. suis* indirect immunofluorescence assays were performed on infected IPEC-J2 cells grown on
218 glass cover slips as described above at dpi 7 and 8. Infected cells on cover slips were washed in
219 PBS, fixed with ice cold methanol for 10 min and subsequently washed twice with PBS.
220 Blocking was performed for 20 min with Superblock® T20 (PBS) blocking buffer (Thermo
221 Scientific) with 1% (v/v) normal goat serum at RT. Primary antibodies (guinea pig TgNuf2
222 (Farrell and Gubbels, 2014); mouse mAb 6-11B-1 acetylated α -tubulin, Invitrogen) were diluted
223 to 1:1000 (v/v) in blocking solution, and incubated for 90 min at 37°C, followed by 2x10 min
224 washes with PBS-Tween 20 (0.01%, v/v), incubation with secondary antibodies diluted 1:600 in
225 blocking solution for 40 min at 37°C, 2x10 min washes with PBS-Tween 20, followed by 1 wash
226 for 5 min in PBS containing 1 μ M DAPI, 4 washes of 5 min at RT with PBS and quick
227 immersion in ddH₂O, before mounting with Aqua Polymount (Fisher Scientific). Mounted
228 samples were hardened for 2-5 days before imaging. A Zeiss LSM 510 Meta with a 63x plan
229 apochromat oil immersion objective was used to collect Z-stacks using ZEN 2009 Light Edition

Comparative apicomplexan cell division

230 (Carl Zeiss Microimaging GmbH, Jena, Germany). Z-stacks were subsequently deconvoluted
231 using Huygens Essential 4.3 software (Scientific Volume Imaging Inc., The Netherlands) with
232 measured point spread functions (PSF) for the respective channels. Z-projections (maximum
233 intensity projections of split channels) were computed with ImageJ 1.48e (National Institutes of
234 Health, Bethesda, MD, USA).

235

236 **2.6 Transmission electron microscopy**

237 For thin-section transmission, pellets of >10% parasitemia *B. bigemina* infected bovine red blood
238 cells were fixed with 2.5% glutaraldehyde in 0.1 M sodium cacodylate (Sigma) buffer (pH 7.4)
239 for 1 hr at RT and processed as described (Nishikawa et al., 2005) before examination with a
240 Philips CM120 Electron Microscope (Eindhoven, The Netherlands) under 80 kV.

241 Pellets of >10% parasitemia *B. divergens* infected human red blood cells were fixed with 2.5%
242 glutaraldehyde 1.25% paraformaldehyde and 0.03% picric acid in 0.1 M sodium cacodylate buffer
243 (pH 7.4) overnight at 4°C. Cells were washed in 0.1 M cacodylate buffer and post fixed with 1%
244 OsO₄/1.5% KFeCN₆ for 1 hr, washed 2x in water, 1x maleate buffer (MB) 1x and incubated in 1%
245 uranyl acetate in MB for 1 hr followed by 2 washes in water and subsequent dehydration in grades
246 of alcohol (10 min each; 50%, 70%, 90%, 2x10 min 100%). The samples were then put in
247 propyleneoxide for 1 hr and infiltrated overnight in a 1:1 mixture of propyleneoxide and TAAB
248 (TAAB Laboratories Equipment Ltd). The following day the samples were embedded in TAAB
249 Epon and polymerized at 60°C for 48 hrs. Ultrathin ~60 nm sections) were cut on a Reichert
250 Ultracut-S microtome, picked up on to copper grids stained with lead citrate and examined in a
251 JEOL 1200EX Transmission electron microscope and images were recorded with an AMT 2k
252 CCD camera.

253

254 **2.7 Phylogenetic analysis.**

255 The following 18S rRNA gene sequences were used: *Cryptosporidium parvum* (GenBank
256 accession no.: L25642.1), *Cryptosporidium muris* (AB089284.1), *Babesia bovis* (L19077.1),
257 *Babesia bigemina* (JQ437261.1), *Babesia divergens* (AJ439713.1), *Babesia duncani*
258 (HQ285838.1), *Babesia microti* (AB219802.1), *Theileria annulata* (EU083801.1), *Theileria*
259 *parva* (L02366.1), *Theileria orientalis* (HM538200.1), *Cytauxzoon felis* (L19080.1), *Theileria*
260 *equi* (KM046918.1), *Hepatozoon canis* (KX712124.1), *Plasmodium falciparum*

Comparative apicomplexan cell division

261 (XR_002966654.1), *Plasmodium berghei* (XR_002688202.1), *Plasmodium vivax*
262 (XR_003001225.1), *Toxoplasma gondii* (L24381.1), *Hammondia hammondi* (KT184369.1),
263 *Neospora caninum* (U03069.1), *Besnoitia besnoiti* (KJ746531.1), *Cystoisospora suis*
264 (KF854251.1), *Sarcocystis neurona* (KT184371.1), *Hyaloklossia lieberkuehni* (AF298623.1),
265 *Goussia janae* (GU479644.1), *Goussia neglecta* (FJ009242.1), *Cyclospora cayetanensis*
266 (XR_003297358.1), *Eimeria callospermophili* (JQ993648.1), *Eimeria tenella* (KT184354.1),
267 *Eimeria necatrix* (KT184349.1), *Eimeria maxima* (KT184346.1), *Eimeria brunetti*
268 (KT184337.1), and *Eimeria acervulina* (KT184333.1). Sequences were aligned using Clustal
269 Omega (Sievers et al., 2011) and a consensus phylogenetic tree was generated using Geneious
270 Prime V2019.1.3 (Invitrogen) using the Jukes-Cantor genetic distance model, neighbor-joining
271 tree build method, bootstrapped 100x using *C. parvum* as outgroup.

272

273 **2.8 Generation of *B. bigemina* IMC1a antiserum**

274 We identified five *B. bigemina* IMC proteins by reciprocal BLASTP searches on EuPathDB
275 (Warrenfeltz et al., 2018) with the 14 *T. gondii* alveolin-domain containing IMC proteins
276 (Anderson-White et al., 2011): PiroplasmaDB.org accession number BBBOND_0204530,
277 BBBOND_0401990, BBBOND_0201220, BBBOND_0208040, BBBOND_0300730). *B.*
278 *bigemina* BBBOND_0204530, which we named BbIMC1a, was most conserved and the whole
279 ORF of 600 bp was synthesized by TwistBioscience (San Francisco, CA), amplified with
280 primers #4831 pAVA-Gibson-Twist-F gaagctcagaccagg and #4832 pAVA-Gibson-Twist-R
281 tgcagaactgttctgtctg to remove the linkers and cloned by Gibson assembly into *PmeI/NruI*
282 digested plasmid pAVA0421 (Alexandrov et al., 2004), expressed as a 6-His tag fusion in
283 *Escherichia coli* BL21-RIPL, purified by Ni-NTA chromatography under denaturing conditions
284 (Invitrogen), refolded, and used to immunize a guinea pig (Covance, Inc). Serum was affinity
285 purified as described previously (Gubbels et al., 2006) against recombinant His6-BbIMC1a.

286

287 **3 Results**

288 **3.1 External budding**

289 Schizogony is defined as: schizo = split (or cleft); gony = birth (genesis of a class of thing). It is
290 generally understood as meaning “multi-fission” and is applied to division modes producing
291 more than two daughter cells per division by peripheral (or cortical) budding from the plasma

Comparative apicomplexan cell division

292 membrane of a polyploid, multi-nucleated mother cell (Fig 2). However, confusion enters with
293 the term “schizont”, which is more widely defined and used to describe any polyploid
294 intermediate cell state regardless of division mode (Fig 4-6): schizo = split (or cleft); -ont = a
295 being (from Greek einai to be) i.e., “to be split”. We forewarn that the term ‘schizont’ is and will
296 be used across division modes for polyploid cells, and thus will not always refer to schizogony
297 per se.

298

299 3.1.1 Schizogony with karyokinesis

300 A wide array of Apicomplexa impacting humans or livestock divide by schizogony, such as
301 nearly all Eimeriidae family members of the Coccidian parasites (Dubremetz, 1973; Joyner and
302 Long, 1974; Dubremetz and Elsner, 1979; Ferguson et al., 2008), the genus of *Plasmodium* in the
303 order of Haemosporida (Arnot et al., 2011; Stanway et al., 2011) as well most (but not all!)
304 piroplasms comprising *Theileria* and *Babesia* spp. (Mehlhorn and Shein, 1984) (Fig 1). The
305 piroplasms are tick-transmitted parasites that multiply in red blood cells without forming
306 pigments (order Achromatorida). Both the piroplasms and the *Plasmodium* spp. (order
307 Chromatorida: form pigments in red blood cells) reside in the clade Haemosporidia for their
308 shared residence within red blood cells. Our discussion here is based mostly on *Plasmodium*
309 schizogony in the red blood cells as it is best studied system, however, insights likely apply
310 widely. A defining principle of schizogony is the disassembly of the mother’s cytoskeleton
311 shortly following completion of host cell invasion, resulting in an amoeboid or pleomorphic cell
312 (Hepler et al., 1966; Gruring et al., 2011) (Fig 2A2) which then undergoes several cycles of
313 DNA replication and nuclear division (Fig 2A3,4). These rounds of DNA replication without
314 budding are controlled by cdc2-related kinase CRK4 which resides in the nucleoplasm and is
315 associated with phosphorylation of the DNA replication machinery (Ganter et al., 2017).
316 Interestingly, the mitotic cycles of the nuclei sharing the same cytoplasm are not synchronous.
317 Mechanistically, this observation is anchored in a differential maturation model of mother and
318 daughter centrosomes following their duplication. Although this model has been firmly
319 demonstrated in higher eukaryotes and is defined by proteins in the centrosome’s distal and sub-
320 distal appendages (Bornens and Gonczy, 2014), it has not been formally confirmed in the
321 Apicomplexa. The last cycle of S/M-phase, in contrast, is synchronous and coupled to the
322 synchronous budding of the daughters at the end of schizogony (Ferguson et al., 2008; Kono et

Comparative apicomplexan cell division

323 al., 2016; Rudlaff et al., 2019) (Fig 2A4,5). Budding follows the activation of the centrosomes’
324 outer-cores, which is always tied to simultaneous centrosome inner-core activation. The exact
325 timing of the nuclear cycle before the onset of budding has not been clearly resolved. Notably,
326 the level of PfCRK4 drops when the budding cycle is about to start, but it is not clear whether
327 this is the defining signal synchronizing the nuclear cycles and/or activating the budding cycle.
328 Potentially, a diffusible signaling protein could respond to the depletion of nutrients, the
329 accumulation of waste, limited space, or act as a quorum sensor, and subsequently synchronize
330 or halt the nuclear cycle before activating the synchronous budding phase. Since the number of
331 offspring varies across *Plasmodium* species, even between different *P. falciparum* strains, across
332 different development stages (e.g. the liver cell expands and produces up to 90,000 merozoites
333 from infection by a single sporozoite (Vaughan and Kappe, 2017)) there is also a strong,
334 programmed genetic component determining the number of offspring (Reilly et al., 2007). Either
335 way, when the ‘commitment to budding’ checkpoint is cleared, the centrosomes that anchor the
336 spindle pole and chromosomes, reorient to associate with the plasma membrane, a step which is
337 mediated by Cyc1 (Robbins et al., 2017). Note that the centrosomes in *Plasmodium* spp.
338 technically are centriolar plaques as these parasites lack canonical centriolar structures.
339 Following plasma membrane docking of the centrosomes, the daughter cytoskeletons start to
340 assemble in connection with the plasma membrane and the buds move outward (Fig 2A4,5). In
341 *P. falciparum* the maturation and release of daughters is mediated by CINCH, a contractile
342 protein in the basal complex (Rudlaff et al., 2019).

343

344 3.1.2 Schizogony with limited karyokinesis

345 Although not separately recognized in the naming conventions, a variation on the classical
346 schizogony as described in the preceding section occurs during sporozoite formation in the
347 invertebrate vector wherein sexual development takes place (Fig 1). This happens in the
348 mosquito midgut for the *Plasmodium* spp (Simonetti, 1996) and in the tick salivary gland for
349 most piroplasms, including *Theileria* spp. and many *Babesia* spp. (Mehlhorn and Shein, 1984;
350 Jalovecka et al., 2018). *P. berghei* and *P. falciparum* sporogenesis have been most extensively
351 studied, which occurs in an extracellular oocyst residing under the basal lamina of the midgut
352 wall (Simonetti, 1996). Like in classical schizogony, the mother’s cytoskeleton is disassembled
353 resulting in a pleomorphic cell. Here, DNA replication and mitosis are not always followed by

Comparative apicomplexan cell division

354 karyokinesis leading to a patchwork of nuclei, with varying levels of ploidity (Fig 2B). Again,
355 the individual nuclei are at different levels of S-phase and mitosis, however, within one
356 polyploid nucleus this cycle is largely synchronous (Howells and Davies, 1971b; a; Schrevel et
357 al., 1977; Sinden and Strong, 1978). Typically, a round of sporogenesis produces thousands of
358 individual sporozoites from a single mother cell. Similar to classical schizogony, the budding of
359 daughters from the cortex occurs simultaneously and is coupled to a synchronized round of S-
360 phase and mitosis (Howells and Davies, 1971a; Schrevel et al., 1977; Araki et al., 2019; Pandey
361 et al., 2019). This process is conserved in *Theileria* and *Babesia* spp. as well, where multiple and
362 multi-lobed nuclei are especially prominent (Moltmann et al., 1983). However, some *Babesia*
363 spp., produce sporozoites through binary fission (Mehlhorn and Shein, 1984).

364 In summary, the intriguing phenomenon is that karyokinesis seems to be optional in these
365 polyploid schizonts. The synchronized cycles of mitosis within a single nucleus suggest that
366 mitotic cycles are organized on the nucleoplasm level just as in classical schizogony, whereas
367 commitment to budding is a factor shared across the whole cytoplasm. How these events are
368 controlled at the molecular level has not been determined.

369

370 3.1.3 Binary and multiple fission

371 Binary fission is defined as “the formation of two daughter cells per division round”. Among the
372 Apicomplexa, binary fission is used to describe the division process in the red blood cell stages
373 of many *Babesia* and *Theileria* parasites. Most *Babesia* spp. form two daughters per division
374 round, i.e. classical binary fission. However, in the red blood cell cycle several clades of
375 *Babesia*, including *Babesia duncani* (Conrad et al., 2006) and *B. microti* (Rudzinska, 1981),
376 form four merozoites per division round (Maltese cross), as do all *Theileria* spp. (Conrad et al.,
377 1985; Conrad et al., 1986; Fawcett et al., 1987; Uilenberg, 2006). This process is known as both
378 schizogony and ‘multiple fission’, however it is generally considered distinct from schizogony,
379 which as mentioned above, is a term historically used when many more daughters are produced.
380 The term “binary fission” does not imply that budding is involved and does not intuitively
381 connect with “multiple fission”, which produces only four daughters per division round, as
382 defined in schizogony. Due to the lack of clarity on how these processes are related and defined
383 cell biologically, the exact nature of *Babesia* cell division in the red blood cell remains to be
384 elucidated. The ambiguity of the used terms (i.e. binary fission, budding, schizogony) to describe

Comparative apicomplexan cell division

385 this process further exacerbates this confusion. In a 1978 publication study using transmission
386 electron microscopy (TEM) the interpretation was as follows (Potgieter and Els, 1977): “The
387 trophozoites were surrounded by a single membrane, were pleomorphic in shape and contained
388 large inclusions of host cell cytoplasm, but no cytostomes or food vacuoles could be identified.
389 Reproduction took place through a process resembling schizogony resulting in the production of
390 two merozoites, the cytoplasmic constituents of the original trophozoite (mother cell) being
391 virtually entirely incorporated into the daughter cells in the process”. In essence, the
392 pleomorphic/ameboid trophozoite in combination with the schizogony reference suggest that the
393 process is conceptually very similar to schizogony, except that term does not capture it since
394 only two daughters are formed. Here we combine existing data with new insights from *in vitro*
395 cultivated *Babesia bigemina* to clarify the mechanistic murkiness surrounding binary fission.

396 *B. bigemina* is a cattle-infecting, tick-transmitted apicomplexan causing vast economic losses
397 (Bock et al., 2004; Suarez et al., 2019). From an experimental point of view, *B. bigemina* cell
398 division is uncomplicated in that it only produces two daughters per division round, and it is a
399 relatively large *Babesia* spp., making it an ideal candidate for microscopy. We focused on the
400 key organizers of cell division: the centrosome (or centriolar plaques) and cortical cytoskeleton.
401 *T. gondii* Centrin1 antiserum on *B. bigemina* showed a specific, albeit relatively weak, signal,
402 but only during daughter budding (Fig 3A). It therefore appears that centrosome composition is
403 dynamic, which was recently also reported for *P. berghei* Centrin4 as this signal was only on the
404 centrosome during mitosis and budding, but not in mature or recently invaded parasites (Roques
405 et al., 2019). In contrast, *Plasmodium* Centrin3 is a popular marker of centrosomes and is always
406 associated with the centrosome, indicating that the dynamics of different Centrins can vary
407 (Mahajan et al., 2008; Kono et al., 2012). We detected microtubules with α -tubulin MAb 12G10
408 generated against ciliate *Tetrahymena thermophila* (Jerka-Dziadosz and Frankel, 1995), which
409 has shown broad reactivity in the Apicomplexa. A spot focused toward the apical end was
410 observed (Fig 3A), but we never observed tubulin in the nucleus, suggesting this antibody does
411 not detect the mitotic spindle. In *Plasmodium* the spindle was successfully visualized with
412 monoclonal antibody B-5-2-1 generated against sea urchin α -tubulin (Gerald et al., 2011), but in
413 *B. bigemina* we observed the same patterns as for MAb 12G10 (not shown). In *T. gondii*,
414 detecting the spindle microtubules has also been challenging, but a polyclonal serum against
415 TgEB1, a microtubule (+)-end binding protein, was very specific for the spindle (Chen et al.,

Comparative apicomplexan cell division

416 2015b). Reactivity of α -TgEB1 in *B. bigemina* across all parasite stages highlighted a spot basal
417 of the apical tubulin staining (Fig 3B). We interpret that EB1 does not bind to the spindle
418 microtubules in *B. bigemina*, but instead associates with the (+)-end of the subpellicular
419 microtubules emanating from the MTOC at the very apical end. This also indicates these
420 microtubules are relatively short and only cover the very apical cap of the parasite. To better
421 visualize the cortical cytoskeletal scaffolds that drive budding we tested polyclonal antisera
422 generated against *T. gondii* IMC proteins (Gubbels et al., 2004; Anderson-White et al., 2011),
423 but unfortunately none showed a signal. Therefore, we generated a specific *B. bigemina* IMC
424 antiserum against BBBOND_0204530, the closest relative to the *T. gondii* alveolin domain
425 containing IMC proteins (Anderson-White et al., 2011), which we named BbIMC1a (Fig S1).
426 IFAs with α -PbIMC1a nicely highlighted the cortical cytoskeleton during budding, extending
427 basally beyond the microtubule signal. In mature parasites we observed signal along the entire
428 length of the merozoite (Fig 3C). In trophozoites we also observed parasites identified by their
429 DAPI signal with weak or variable intensities of either the IMC1a or tubulin signals that
430 appeared disorganized, or at least not to outline a merozoite (Fig 3C top panel and middle panel
431 marked by an asterisk). We interpreted these amorphous signals to represent trophozoites that are
432 at the stage between invasion and the start of cell division. However, across all parasites in
433 division we observed parasites forming next to each other, with apical ends emerging first with
434 V-shape symmetry.

435 To obtain a higher resolution of the mechanistic steps in the *B. bigemina* division process we
436 performed TEM. We focused on stages after the parasites escaped from their vacuole and entered
437 G1 growth phase (trophozoites). We observed a high frequency of zoites wherein the IMC
438 breaks into 5-6 pieces, still in curved structures on the edge consistent with an ameboid or
439 pleomorphic status for the zoites (Fig 3D1). This consistent observation suggests that
440 disassembly of the mother cytoskeleton is spatially organized resulting in a symmetrical
441 appearance, which reflect the trophozoites identified by IFA (Fig 3C). Similar observation on
442 disassembling mother IMC have been reported for *Plasmodium* ookinetes in the mosquito
443 midgut (Carter et al., 2007), and for sporozoites in liver cells, where regularly spaced breaks
444 occur in the IMC, although not quite as symmetrically organized as seen here in *B. bigemina*
445 (Jayabalasingham et al., 2010). In a budding zoite two daughter buds are emerging on one side of
446 the cell (like rabbit ears), and not on polar opposites (Fig 3D2). The shape of the nucleus is also

Comparative apicomplexan cell division

447 consistent with the anchoring of the nucleus at the apical end of the daughters, which, by using
448 other division modes as a guide, we assume is through the spindle poles (Potgieter and Els,
449 1977). For the growing stages, we captured many transverse cross sections of two side-by-side
450 budding daughters with the nucleus at various stages of division (Fig 3D 3-5). Finally,
451 completely formed daughters appear side by side under a similar angle as the early daughter buds
452 (compare the orange arrows in Fig 3D2 with 3D6). Additional TEM images of *Babesia* buds in a
453 V orientation consistent with our data have been reported elsewhere (Friedhoff and Scholtyseck,
454 1977; Potgieter and Els, 1977; Scholtyseck, 1979). A section through the basal ends of still
455 connected *Babesia divergens* parasites (predominantly a cattle parasite but opportunistic in
456 humans) displays an electron dense structure on the basal end of the IMC consistent with a basal
457 complex (Fig 3E). Although we did not capture a section through this structure in *B. bigemina*, a
458 similar appearance of the basal complex in *B. bigemina* has been reported previously (Potgieter
459 and Els, 1977).

460 Overall, the budding of daughters in *B. bigemina* shares many features seen across asexual
461 apicomplexan development (Fig 3F). First, the angle between the daughter buds fits with the
462 pleuromitosis (closed mitosis with the spindle poles in close proximity at one side of the nucleus)
463 model dictated by closely apposed centrosomes at the apically defining side of the nucleus. This
464 is observed across the Apicomplexa that have been studied (Gerald et al., 2011; Francia and
465 Striepen, 2014). As a result, daughter buds are formed next to each other rather than in opposing
466 orientations (middle panel Fig 3F3-5). The *B. bigemina* trophozoite has an ameboid appearance
467 after invasion and cytoskeleton is disassembled (Fig 3E1, 3F2; and (Potgieter and Els, 1977)),
468 which likewise is observed during the corresponding stage of *P. falciparum* (Gruring et al.,
469 2011). Taken together, these data firmly illustrate that the processes known as binary fission and
470 schizogony, and by extension multiple fission as seen in *Theileria* spp., are mechanistically the
471 same and only differ in the number of nuclear replication cycles before the onset of cytokinesis.
472 Collectively, we now group these division forms together under the umbrella “external (aka
473 cortical) budding”
474

475 3.1.3 Other variations on cortical budding

476 Schizogony by cortical budding as described in the preceding sections are found in various
477 asexual stages. Other forms on cortical budding can be found in sexual development stages,

Comparative apicomplexan cell division

478 which we will briefly highlight here to illustrate the spectrum of division modes. *Plasmodium*
479 male gametocytogenesis produces flagellated microgametes in a process known as
480 “exflagellation”. This process occurs in the red blood cell and unfolds by several fast rounds of
481 S/M-phase resulting in a single polyploid nucleus (Sinden et al., 1978; Sinden, 1983). The
482 cortical ‘budding’ of microgametes, which at the cytoskeletal level basically are a single
483 flagellum and only contain microtubules, progresses while the nuclear material partitions.
484 Interestingly, a recent study using Ndc80 as a marker for the kinetochores demonstrated that the
485 genome size universally increases to 8N, but that chromosome replication is asynchronous
486 (Pandey et al., 2019). This is in contrast to what is observed during asexual schizogony, where
487 the rule is that the mitotic cycles are synchronous within a shared nucleoplasm.

488 In addition, microgametocyte formation of *T. gondii* also progresses through a cortical
489 budding process (Ferguson et al., 1974). As discussed in detail below, it is salient to note that the
490 asexual division of *T. gondii* is by internal budding, not through cortical budding. *T. gondii*
491 microgametocytes formation plays out by the association of 1N nuclei in a multi-nucleated
492 microgamont with plasma membrane of the mother cell. Interestingly, the mother cell
493 (macrogamont) maintains an IMC where in holes are present to facilitate association of the
494 nuclei with the plasma membrane. From here, bi-flagellated microgametes bud outward in a
495 cortical budding process (Ferguson et al., 2008). Interestingly, this process is conserved across
496 the Coccidia, as it is also reported for *Eimeria* spp. which, in contrast to *T. gondii*, replicate
497 asexually by schizogony (Ferguson et al., 1980) (Fig 1). Taken together, the notable features here
498 are maintenance of the cortical cytoskeleton (Dubey et al., 2017) in combination with cortical
499 budding while S-phase, mitosis and karyokinesis have been completed before the onset
500 ‘budding’.

501

502 **3.2 Internal budding**

503 **3.2.1 Endodyogeny**

504 Endodyogeny is defined as: endo = inner/internal; dyo = two; geny = genesis, meaning birth;
505 production/generation/origin. This term is applied to a type of reproduction in which two
506 daughters are formed within a parent cell (Goldman et al., 1958; Sheffield and Melton, 1968).
507 Endodyogeny has been described in detail for *T. gondii* tachyzoites (Nishi et al., 2008;
508 Anderson-White et al., 2012) and is employed as well by its closest evolutionary neighbors

Comparative apicomplexan cell division

509 comprising several genera of the Sarcocystidae (Fig 1, 4). These include *Hammondia*, *Neospora*
510 and *Besnotia* spp. as well as the tissue cyst-forming stages of *Sarcocystis neurona*. During
511 endodyogeny, the mother's cytoskeleton is not disassembled following completion of invasion,
512 and two daughter buds assemble on centrosomes residing within the cytoplasm. Only at the very
513 last stage of daughter budding is the mother's cytoskeleton disassembled and is the plasma
514 membrane deposited on the new daughters, which is mediated by recruitment of the "gliding
515 motor complex" to the IMC. This complex contains a multi-acylated protein glideosome
516 associated protein, GAP45, that is anchored in both the plasma membrane and the IMC outer
517 membrane and 'zippers' these structures together in an apical to basal direction (Gaskins et al.,
518 2004; Frenal et al., 2014). Many of the cell cycle checkpoints throughout endodyogeny have
519 been resolved. Specifically, two checkpoints have been described upon commitment to mitosis
520 and budding, one likely dedicated to mitosis and the other to budding. This is thought to facilitate
521 the uncoupling of S/M cycles from budding in the multi-daughter division modes and
522 differentially activate the centrosome inner- and outer-cores (Suvorova et al., 2015; Naumov et
523 al., 2017; White and Suvorova, 2018). Like in schizogony, daughter budding occurs in sync with
524 S/M-phase and karyokinesis. Upon emergence of daughters, a narrow cytoplasmic bridge at the
525 basal end remains connected with a residual body containing remnants of the mother cell, which
526 will be largely resorbed into the daughters (Frenal et al., 2017b; Periz et al., 2019). As a result,
527 the daughter parasites remain in contact with each other and could therefore have the false
528 appearance of endopolygeny. To differentiate these two processes, this division process has been
529 referred to as 'repeated endodyogeny'.

530

531 3.2.3 Endopolygeny

532 Endopolygeny is defined as: endo = inner/internal; poly = multiple; geny= genesis/birth. This
533 term is used to describe the reproduction types wherein more than two individuals are formed
534 simultaneously within the cytoplasm (i.e. not from the cortical periphery) of a polyploid parent
535 cell. One of the key features of internal budding is that the mother's cytoskeleton is maintained
536 throughout cell division and only disassembles just before the emergence of almost completely
537 assembled daughters. Although not differentiated in the naming conventions, two sub-forms can
538 be distinguished: either the polyploid mother cell can be multinucleate, or it can contain one
539 large polyploid nucleus depending on whether karyokinesis follows each round of S-phase. Both

Comparative apicomplexan cell division

540 these forms of budding are found within the tissue cyst-forming Coccidia, more specifically the
541 Sarcocystidae (Fig 1, 5, 6). These division forms are related to endodyogeny, since the mother's
542 cytoskeleton is maintained throughout the division cycle until the maturation of the daughter
543 cells. We define these three forms here collectively as “internal budding”. Internal budding by
544 the Sarcocystidae is unique among the Coccidia as other families, notably the closely related
545 Eimeriidae, replicate by schizogony (Fig 1). Two emerging systems exist to study the variations
546 in progression of endopolygeny: *Sarcocystis neurona* is a model for studies representing the
547 form without completing karyokinesis (Fig 5) (Vaishnava et al., 2005; Dubey et al., 2017),
548 whereas merogony of *Cystoisospora suis* provides an accessible *in vitro* model for the form
549 including karyokinesis after each S/M-round (Fig 6) (Worliczek et al., 2013).

550

551 3.2.3.1 Endopolygeny with karyokinesis

552 *C. suis* is the causative agent of suckling piglet coccidiosis (Shrestha et al., 2015). Although
553 phylogenetically *C. suis* falls within the cyst-forming Coccidia (Fig 1), tissue cysts have never
554 been observed and the known coccidian development cycle is monoxenic in pigs: the absence of
555 tissue cyst forming capacity is likely a secondary loss in this species (Stuart et al., 1982; Shrestha
556 et al., 2015). *C. suis* asexually replicates in epithelial cells of the porcine small intestine by
557 endodyogeny and endopolygeny, depending on the generation of asexual stages (alternatively
558 called types: meronts/merozoites type I, II and subtype II (Matuschka and Heydorn, 1980). Early
559 asexual division after infection of the gut epithelium is restricted to endodyogeny (often in
560 consecutive cycles within one parasitophorous vacuole, i.e. ‘repeated endodyogeny’), whereas
561 endopolygeny is described from day 3-4 post infection onwards *in vivo* (Lindsay et al., 1980;
562 Matuschka and Heydorn, 1980) and from day 7 onward *in vitro* (Worliczek et al., 2013),
563 concurrent with cells replicating by endodyogeny.

564 As for *B. bigemina*, we tracked *in vitro* progression of *C. suis* development using the
565 toolbox of reagents we established for *T. gondii*. In *C. suis* zoites undergoing endopolygeny, the
566 mother's subpellicular microtubule cytoskeleton is clearly visible in large polyploid cells as an
567 apically concentrated microtubular accumulation joined in the mother's conoid (Fig 5A-D). This
568 confirms the mother's cytoskeleton is maintained throughout endopolygeny. To track the
569 progression of S/M-phase across the nuclei we used the kinetochore component Nuf2 (Farrell
570 and Gubbels, 2014) in combination with acetylated α -tubulin, which marks the spindle poles

Comparative apicomplexan cell division

571 during mitosis (note that spindle microtubules disassemble during interphase (Farrell and
572 Gubbels, 2014; Chen et al., 2015b)). The first observation is that the status of mitosis (spindle
573 visible by tubulin stain) and the status of kinetochore separation varies among nuclei within the
574 same cell (Fig 5A, B). Furthermore, it is evident that parasites expand non-geometrically, as
575 counted by spindle poles per nucleus varying from 3, 4, 5, to 6 are seen in Fig 5A and B, whereas
576 12 budding daughters, i.e. non-geometrically expanded, can be discerned in Fig 5C, D. These
577 two observations indicate that the nuclear division cycles are not synchronous, which is
578 consistent with expansion numbers described in the literature (e.g. (Lindsay et al., 1980;
579 Matuschka and Heydorn, 1980)). Here we show for the first time that this is associated with
580 asynchronous nuclear replication cycles. Finally, we show that the final round of mitosis is
581 synchronous for all nuclei and is coupled with daughter budding, as seen in schizogony. Our
582 insights are summarized in the schematic of Fig 5E. Based on the details revealed here, we
583 conclude that like in schizogony, the S/M-phase progression are controlled at the nuclear level,
584 most likely differing maturity of the mother and daughter centrosomes, but that the commitment
585 to budding is synchronized across the cytoplasm.

586 Reports on *T. gondii* endopolygeny suggest geometric expansion of nuclei: 8–16 progeny per
587 endopolygeny replication cycle in the cat gut have been observed (Ferguson et al., 1974).
588 Historically, the sexual cycle of *T. gondii* has been poorly experimentally accessible, but *in vitro*
589 completion of the sexual cycle in cat intestinal organoids was recently reported, which is
590 expected to provide experimental accessibility (Martorelli Di Genova et al., 2019). To date, *T.*
591 *gondii* endopolygeny studies have not been so comprehensive to support a strong conclusion in
592 this matter.

593 An additional notable observation in Fig 5A is the presence of multiple parasites within a
594 single vacuole undergoing endopolygeny. It has been described before that several multinucleate
595 meronts can be present in a single vacuole, which indicates that more than one asexual division
596 occurs in the same cell (Lindsay et al., 1980). As such, this reveals that multiple rounds of
597 budding within the same vacuole are not exclusively found during endopolygeny as described
598 above for *T. gondii*. This phenomenon therefore highlights that the timing of budding is
599 determined by a genetic program, and not controlled by environmental factors, which we also
600 concluded for schizogony.

601

Comparative apicomplexan cell division

602 3.2.3.1 Endopolygeny without karyokinesis

603 *S. neurona* has a sylvatic cycle in the Americas with small mammals as intermediate hosts and
604 the opossum as the definitive host. However, accidental infection of horses can cause equine
605 protozoal myeloencephalitis (EPM) (Reed et al., 2016). Using the same strategy as mentioned
606 above, we observe an apical concentration of microtubules across cells with progressively larger
607 single nuclei indicating the mother's cytoskeleton is maintained throughout endopolygeny
608 (arrowheads in Fig 6A). Furthermore, the *S. neurona* IMC can be visualized through
609 overexpression of TgIMC15-YFP, which highlights the sutures in the IMC of the mother
610 throughout development (Fig 6B) (Dubey et al., 2016). When the cell prepares for budding
611 IMC15 also appears on the centrosomes at which point the mother's IMC is still prominently
612 present (Fig 6B2). Only at the conclusion of the budding process is the mother's cytoskeleton
613 disassembled, which mimics the dynamics of the IMC during *T. gondii* endodyogeny (Anderson-
614 White et al., 2011; Dubey et al., 2016).

615 In contrast, to *C. suis*, the S/M cycles of *S. neurona* are completely synchronized: in Fig 6A2
616 we observe a cell in interphase characterized by absence of spindle microtubules, whereas the
617 right cell displays spindle microtubules associated with each centrosome. This confirms previous
618 observations (Vaishnav et al., 2005), and indicates that when the nucleoplasm is shared, the
619 individual status of centrosome maturation is overruled, likely by a factor diffusing in the
620 nucleoplasm. Late in development the large polyploid 32N nucleus shifts into a multi-lobed,
621 'serpentine' morphology (Fig 6A3), which sets the stage for a final round of S/M-phase now
622 coupled to karyokinesis and internal budding resulting in 64 daughters (Fig 6A4). Thus, when
623 the S/M-phase are not followed by karyokinesis the nuclear cycles remain synchronized and
624 progeny number are the result of geometric expansion.

625

626 3.2.4 Budding without multiplication and multiplication without budding

627 The spectrum of division modes not yet covered spans two more manifestations in sexual
628 development stages. The first, budding without multiplication, is the formation of kinetes in the
629 Heamosporidia. The *Plasmodium* spp. generate ookinetes from a fertilized zygote (ploidity of 2-
630 4N in a single nucleus) that cross the mosquito gut wall (reviewed in (Angrisano et al., 2012;
631 Bennink et al., 2016)). Although the zygote lacks a cortical cytoskeleton, the ookinete has a
632 complete cortical cytoskeleton comprising IMC and cortical microtubules. This cortical

Comparative apicomplexan cell division

633 cytoskeleton is formed by the ookinete through from the cortex of the zygote in absence of
634 karyokinesis, though a budding stage dubbed 'retort' (Canning and Sinden, 1973; Carter et al.,
635 2007). Yet even more exotic variations occur in the piroplasms; both *Theileria* and *Babesia* spp.
636 produce kinetes, which do not bud from the cortex, but into an internal vacuole formed inside the
637 zygote (see (Mehlhorn and Shein, 1984) for a detailed review). Thus, cortical budding can be
638 uncoupled from the nuclear cycle in the zygote stages.

639 The second variation is multiplication without budding, of which there are three different,
640 possibly related examples. The first is found in the *Babesia* spp. kinetes, which following their
641 formation in the tick gut, cross the midgut and migrate to the tick ovary. Here, the cortical
642 cytoskeleton disassembles and the cell transforms into a pleomorphic cell (Moltmann et al.,
643 1982; Mehlhorn and Shein, 1984). Subsequently, several rounds of S/M-phase without
644 karyokinesis occur to produce a multiploid, lobed nucleus. In a process not understood at neither
645 the mechanistic nor molecular level, these large cells divide into multiple cells, each with a
646 single nucleus. Surprisingly, neither the mother nor the daughter cells have a cortical
647 cytoskeleton. This indicates that at this life stage cell division is independent of any form of
648 budding, and thus indicates that in Apicomplexa the cortical cytoskeleton is not a strict
649 requirement for cell division. From each of these pleomorphic cells a new kinete then forms by
650 budding mediated by cortical cytoskeleton formation into an internal vacuole as described above.
651 The released kinetes then migrate to the salivary glands where they undergo sporogenesis.

652 The second example of multiplication without budding is a binary variation on the above
653 process found in some *Babesia* spp. (Mehlhorn and Shein, 1984). Kinetes that invaded the tick
654 salivary gland disassemble their cytoskeleton and undergo one round of S/M-phase, karyokinesis
655 and cell division. However, no cortical cytoskeleton is assembled during these binary division
656 rounds. The cortical cytoskeleton is reportedly assembled slowly during the last couple of
657 division rounds resulting in mature sporozoites. Thus, the salient details are that this process is
658 binary and appears to be efficient with resources as the cytoskeleton is only assembled in the last
659 round (unlike endodyogeny, where a complete parasite is assembled each multiplication round).
660 This process has been described for *B. canis* (Schein et al., 1979), a dog parasite, and *B. bovis*
661 (Potgieter and Els, 1976), a cattle parasite, but likely occurs widely across *Babesia* spp.
662 exclusively replicating by binary fission in the red blood cell (Fig 1) (Mehlhorn and Shein,
663 1984). Thus, across all life stages, these particular *Babesia* parasites seem to have lost the ability

Comparative apicomplexan cell division

664 to produce more than two daughters per division round, providing a model system to unravel the
665 specifics of the genetic program and regulatory network.

666 The third example is the process of sporoblast formation in the Coccidia. This occurs within
667 the oocysts released into the environment. Depending on the species, the zygotes can divide
668 themselves into 2 to 4 sporoblasts (this number is a defining feature in diagnosis of fecal oocysts;
669 not dividing is an option as well (Gardiner et al., 1998)). Inside the sporoblasts 2-4 sporozoites
670 form through a budding mechanism coupled to DNA replication. Although studied in many
671 parasites, *T. gondii* produces two sporoblasts and four sporozoites per sporoblast and as such is
672 the simplest form. Consistent with EM data (Ferguson et al., 1979a), it was recently shown that
673 neither microtubules nor IMC proteins were involved in *T. gondii* sporoblast formation (Dubey
674 et al., 2016). Considering the process and life stage, this process therefore appears akin to kinete
675 multiplication in *Babesia* spp., as described above. This thus seems to connect these two
676 parasites across a large phylogenetic distance, which begs the question whether this is an
677 ancestral connection, or a case of convergent evolution.

678

679 **4. Discussion**

680 The picture of cell division across all life stages of the Apicomplexa is that principle differences
681 exist between the sexual and asexual cell division strategies. In the sexual stages, cell number
682 expansion is not necessarily related to budding a daughter cytoskeleton. This shows that budding
683 is in principle not required for apicomplexan cell division, but there are very few mechanistical
684 or molecular details available for these division modes. The other insight is that all invasive
685 zoites with an apical complex form by a budding strategy, which is initiated and coordinated by
686 the centrosome's outer-core and proceeds in an apical to basal assembly direction. In all the
687 asexual life cycle stages zoite budding is coupled to a complete nuclear cycle (S/M-phase plus
688 karyokinesis). Another general rule across asexual development is that budding is synchronized
689 across the whole cell. This indicates that the centrosome outer-core activation is always coupled
690 to inner-core activation in asexual stages on a shared cytoplasm-wide level (e.g. a diffusible
691 kinase or kinase substrate). The exceptions to this rule are only found in sexual stages:
692 microgametocytogenesis and (oo)kinete formation in the Haemosporidia.

693 Besides these general rules, there are several variations within asexual division modes which
694 partition into two mechanistically different strategies: internal budding and external budding (Fig

Comparative apicomplexan cell division

695 1). Internal budding comprises endodyogeny and the two variations on endopolygeny, whereas
696 external budding captures the two variations on schizogony, binary fission, and multiple fission.
697 The number of offspring in each strategy can vary from two (endodyogeny and binary fission) to
698 several orders of magnitude higher ($>10,000$ in schizogony). At the furthest extreme are several
699 bovine-infecting *Theileria* spp. of which the schizonts in the white bloods that trigger
700 transformation of their lymphocyte host cells (i.e. leukemia) resulting in division and expansion
701 of the parasites schizont stage along with their host cell (Luder et al., 2009; Chakraborty et al.,
702 2017). As remarked throughout, the number of daughter cells per division round in each life
703 stage is largely genetically controlled, but the details on the controls are just starting to emerge.

704 Overlapping with the genetic switch committing to budding is the bi-partite centrosome
705 cycle. The apicomplexan centrosome and mitotic cycles are controlled by Nek and Aurora
706 kinases (Reininger et al., 2011; Carvalho et al., 2013; Chen and Gubbels, 2013; Berry et al.,
707 2016; Berry et al., 2018). In *T. gondii* it has been demonstrated that the switch from solely a
708 nuclear cycle to a combined nuclear and budding cycle is controlled by a MAP kinase-like
709 protein (Brown et al., 2014; Sugi et al., 2015; Suvorova et al., 2015). Ultimately, cell cycle
710 progression and the activation of each core is regulated by cyclin and CDK pairs adapted to each
711 apicomplexan cycle, as they likely act independently on the inner- and outer-centrosome cores
712 (Le Roch et al., 2000; Merckx et al., 2003; Alvarez and Suvorova, 2017; Ganter et al., 2017;
713 Naumov et al., 2017; Robbins et al., 2017; White and Suvorova, 2018). An open question is the
714 identity on the factor(s) controlling the pause of nuclear cycles across parasites prior to the final
715 round of coupled S/M-phase and budding in the polynucleate division modes.

716 The control of the nuclear cycle appears to depend on the ploidy of the nucleoplasm. When
717 each S/M-phase is followed by karyokinesis, then the cycles of individual nuclei are diverging.
718 Mechanistically, this observation is anchored in differential maturation of mother and daughter
719 centrosomes following their duplication; the mother centrosome is sooner primed for another
720 round of replication. This mechanism has been firmly demonstrated in higher eukaryotes and is
721 defined by proteins in the centrosome's distal and sub-distal appendages (Bornens and Gonczy,
722 2014). However, this has not been directly demonstrated yet for the apicomplexan centrosome
723 (Morlon-Guyot et al., 2017; Courjol and Gissot, 2018; Chen and Gubbels, 2019). At first sight,
724 contrasting insight comes from synchronized endodyogeny observed in *T. gondii* tachyzoites.
725 Upon completion of cell division, *T. gondii* daughters stay connected through a cytoplasmic actin

Comparative apicomplexan cell division

726 bridge maintained by Myosin I (Frenal et al., 2017b; Periz et al., 2017). If this bridge is intact, all
727 conjoined tachyzoites undergo endodyogeny in synchrony resulting in geometric expansion
728 numbers. However, the cell division cycles of parasites sharing the same vacuole become
729 uncoordinated if the bridge is disrupted. Strengthening this conclusion is the observation that 4-
730 5% of tachyzoites by chance form multiple (3-4) daughters per division round: the timing of
731 daughter budding is still synchronized with the other parasites in the vacuole despite the fact that
732 these tachyzoites have undergone two rounds of S/M phase (Hu et al., 2004). For signaling
733 purposes, these paradoxical “multi-daughter endodyogenic” parasites are still in the
734 synchronized cycle of “S/M coupled to budding” state consistent with endodyogeny.
735 Accumulating insights from various mutants displaying increased incidences of “multi-daughter
736 endodyogenic” parasites (Dubey et al., 2017) suggests that such parasites fail to start budding
737 because they are missing membrane building blocks to assemble the daughter IMC, and then slip
738 into the next cell cycle while remaining in the “S/M coupled to budding” state.

739 When karyokinesis does not follow each S/M phase polyploid nuclei are formed. In *S.*
740 *neurona* endopolygeny, karyokinesis does not occur at all till the onset of budding, but in
741 Hemosporidiosis sporogenesis, karyokinesis is more optional, which leads to a mix of nuclei
742 with various levels of ploidy. However, the mitotic cycle within each nucleoplasm appears to be
743 coordinated (Gerald et al., 2011; Roques et al., 2015), suggesting this level of control is not at the
744 centrosome level, but likely the chromatin or nucleoplasm level. The control and mechanism of
745 karyokinesis are not understood, which is also the case in well-studied model eukaryotes
746 dividing by closed mitosis such as *Aspergillus nidulans*, fission yeast, and baker’s yeast. The
747 challenge in polyploid nuclei is to keep the multiple sets of chromosomes together so they can be
748 accurately partitioned into the daughters. The solution is that the chromosomes remain clustered
749 throughout the cell cycle by tethering the centromeres to the nuclear lamina. For instance, in *T.*
750 *gondii* the 13 centromeres and associated kinetochores remain clustered at the centrocone, a
751 nuclear envelope fold that houses the spindle microtubules during mitosis (Brooks et al., 2011;
752 Farrell and Gubbels, 2014). Similar observations have been made throughout the *Plasmodium*
753 life cycle using kinetochore markers (Pandey et al., 2019). Strayed chromosomes are rarely
754 observed but individual centromeres are seen during interphase in the *Plasmodium* schizogony in
755 the red blood cell. However, all centromeres cluster together again at the spindle pole before
756 entering mitosis (Hoeijmakers et al., 2012). Clearly, centromere clustering and sequestration at

Comparative apicomplexan cell division

757 the nuclear envelope through the kinetochores is an effective strategy to warrant that complete
758 sets of chromosomes are maintained in polyploid nuclei.

759 None of the above addresses why there are two different forms of budding; i.e. internal vs
760 external. We will try to address this by looking at the phylogeny. The first question is whether
761 either internal budding or external budding are an innovation or ancestral process. Since not
762 enough cell division details are known for Apicomplexa outside those groups included in Fig 1, a
763 firm answer is not possible. In favor of loss of internal budding is the generally more reduced
764 genome and streamlined biology found in the *Plasmodium* spp. and the piroplasms (e.g. host cell
765 invasion (Gubbels and Duraisingh, 2012)). Alternatively, in favor of innovation of internal
766 budding in the cyst-forming Coccidia is the putative advantage evidenced during *T. gondii*
767 endodyogeny. In this case, the mother parasite remains invasion- and egress-competent
768 throughout most of the replication cycle, hence increasing the resilience of the parasite in the
769 dynamic host system (i.e. immune attacks) to move between host cells (Gaji et al., 2011). In
770 contrast, during *S. neurona* endopolygeny the micronemes disappear halfway through the
771 division process, which depletes their invasion capacity (Vaishnava et al., 2005); hence, this
772 model does not hold true for the polyploid internal budding modes. Alternatively, it can be
773 argued that the maintenance of a cortical cytoskeleton in the mother makes the parasites more
774 resistant to mechanical stress, but it is not immediately obvious how this sets the tissue cyst-
775 forming Coccidia apart from parasites dividing by external budding. As all of the Coccidia have
776 oral transmission routes, each species exhibits asexual stages in gut epithelial cells; indeed, the
777 non-cyst forming Coccidia complete their whole cycle in the intestinal epithelium. This
778 revelation suggests that the differentiation of internal from external budding might be coupled to
779 the innovation of tissue cyst formation. The requirements for cyst formation comprise dispersion
780 throughout the host beyond the gut-epithelium and assembly of the cyst in neuronal and/or
781 muscular tissue, which do not have obvious links to division modes. Both the tissue cyst
782 inhabiting bradyzoite stages of *T. gondii* and *S. neurona* (pre-bradyzoite metrocytes as well)
783 undergo endodyogeny; only the acute stage of *S. neurona* divides by endopolygeny (Dubey et
784 al., 2001). In addition, although the acute stage of *S. neurona* dissolves the vacuolar
785 compartment and replicates in the host cell cytoplasm, bradyzoite multiplication and cyst
786 formation occur within a vacuole (Jakel et al., 2001). Cyst expansion has to occur gradually so as
787 not to compromise the cyst wall, which obviously is more compatible with endodyogeny than

Comparative apicomplexan cell division

788 endopolygeny. Notably, bradyzoite replication within *T. gondii* cysts is asynchronous and is
789 consistent with this model (Watts et al., 2015).

790 An outlier is *Eimeria callospermophili*, a rodent parasite that replicates by endopolygeny
791 rather than schizogony, and as far as known, does not form tissue cysts (Roberts et al., 1970;
792 Hammond, 1973). *E. callospermophili* undergoes several rounds of S-phase that are each
793 followed by karyokinesis to produce 4-10 nuclei per schizont while the mother's cytoskeleton is
794 maintained. In synchrony, two daughters per nucleus bud internally and the plasma membrane is
795 acquired when the daughter are about 1/3 developed, resulting in 8-20 merozoites. This suggests
796 internal budding was likely present before the advent of tissue cyst formation. However, the
797 phylogenetic position of this parasite is on the edge of the *Eimeria* spp. (Fig 1). To complicate
798 matters further, genome information has demonstrated that the *Eimeria* spp. and the *Isopora* spp.
799 branch within each other and that neither are monophyletic clades (Kvicerova and Hypsa, 2013).
800 Furthermore, the mechanism of cortical budding occurs across the Coccidia sexual cycle during
801 microgametocyte formation (Ferguson et al., 1974; Ferguson et al., 2008). Hence, parasites can
802 exhibit both cell division modes at different stages of their life-cycles – internal and external
803 budding. We also know that sporozoite formation in *T. gondii* occurs through an internal budding
804 mechanism in the absence of a maternal cytoskeleton (Ferguson et al., 1979b; Dubey et al.,
805 2017). Interestingly, the timing of plasma membrane association with the cytoskeleton is much
806 earlier in this situation compared to the other asexual stages occurring in presence of a maternal
807 cytoskeleton, which indicates the timing of events is flexible. Taken together, there appears to be
808 a continuum between the morphogenic features of the Coccidia, suggesting that there is a
809 significant level of plasticity in biology and division modes. Further insights may result from the
810 investigation of parasite species straddling the two division modes; for example, the *Goussia*
811 spp. bridging the cyst-forming and non-cyst forming Coccidia (Fig 1) (Barta et al., 2001). The
812 *Goussia* spp. are found in fish, reptiles and amphibians, which have not been extensively studied
813 at the cell biological level (Rosenthal et al., 2016). Overall, why the two different extant forms of
814 budding exist cannot be answered with satisfaction based on the factors we considered.

815 This leaves the question of what the mechanistic differences are between internal and
816 external budding. The key question here is how parasites transitioned between the general
817 strategies of external vs internal budding. A principal difference is rooted in the localization of
818 the centrosome. In cortical budding the centrosomes reorient to the plasma membrane, whereas

Comparative apicomplexan cell division

819 during internal budding they remain in the cytoplasm. A simple model suggests that the presence
820 of the mother's cytoskeleton physically prevents access of the centrosome to the plasma
821 membrane. Yet, it is unlikely such a simplistic model fully describes this complicated process. A
822 structure anchoring the centrosome to the cortical cytoskeleton has been described for *T. gondii*
823 endodyogeny; a striated fiber assemblin (SFA), extending from the centrosome to the conoid
824 (Francia et al., 2012). SFA fibers are typically found in the flagellar assembly of algae, where
825 they contribute to orientation of the basal body rootlet system relative to other subcellular
826 structures (Francia et al., 2015). During *Eimeria necatrix* schizogony, a dense structure anchors
827 the centrosome to the plasma membrane. This structure migrates basally along with the cortical
828 microtubules during the progression of daughter bud assembly (Dubremetz, 1975), and might be
829 related to the SFA fiber. Such a structure has not been described for *Plasmodium* schizogony in
830 the red blood cell, although the SFA genes are conserved in *Plasmodium* spp. (Lechtreck, 2003).
831 Thus, SFA-like structures anchoring the centrosome to the plasma membrane have been
832 observed in *Eimeria* schizogony (Dubremetz, 1971) and even in *Theileria equi* sporozoite
833 schizogony (Moltmann et al., 1983) and appear to be a differentiating factor between internal and
834 external budding. Further study of SFA genes across the Apicomplexa may reveal the nature of
835 how nuclei are anchored in the buds across the different division modes.

836 Several more principle difference between internal budding relative to cortical budding exist.
837 For example, the mother and daughter cytoskeletons must be differentially stabilized upon
838 completion of budding. What are the putative mechanisms? It has been shown that a timely
839 regulated proteolysis which removes the C-terminus of the major network component, IMC1,
840 coinciding with conversion of the network from a detergent-labile to a detergent-resistant state
841 late in *T. gondii* daughter cell development (Mann et al., 2002). On the other hand, ubiquitination
842 of the mother's cytoskeleton marks it for destruction (Silmon de Monerri et al., 2015; Dhara and
843 Sinai, 2016). Although the former informs about maturation and the latter about destabilization,
844 neither informs directly on the basis of differential stability. In parallel, some of the maternal
845 building blocks (e.g. IMC proteins, glideosome) are recycled in the final growth spurt of the
846 daughters (Ouologuem and Roos, 2014; Periz et al., 2019). An additional mechanism is provided
847 by differential components present on either mother (e.g. MSC1b (Lorestani et al., 2012),
848 GAP45 (Gaskins et al., 2004), or IMC7, 12, 14, 17, 18 and 20 (Anderson-White et al., 2011;
849 Chen et al., 2015a)) or daughter parasite (e.g. IMC16, 29 (Chen et al., 2015a; Chen et al., 2016)),

Comparative apicomplexan cell division

850 or swapping places from mother to daughter (e.g. SPM3, (Samad et al., 2015)). Such differential
851 composition of mother and daughters may be factors in differential stability, but to date no single
852 factor provides a satisfactory explanation.

853 Another potential problem posed by the mother's cytoskeleton during internal budding
854 occurs in the growth phase, where it restricts access to nutrients and complicates the ability to
855 expel waste. This is most relevant for the expanding cell during endopolygony with large
856 cytoplasmic mass. Although both the apical and basal extremes of the cytoskeleton have
857 openings toward the plasma membrane, they are relatively small and it is not clear whether they
858 are sufficient for the level of exchange needed. However, it is not clear whether the sutures
859 between the alveoli are permeable for diffusion of small molecules, which would void this
860 argument. Either way, a set of apical annuli largely composed of AAP proteins residing in the
861 IMC sutures were recently suggested to function as pores across the IMC (Engelberg et al., 2019;
862 Lentini et al., 2019). In support of this hypothesis is the narrow conservation of AAP protein
863 orthologs only in the Sarcocystidae, indicating their function is most likely in support of internal
864 budding. However, disruption of apical annuli structure resulted in a minor fitness loss of *T.*
865 *gondii* tachyzoites, which might be because endodyogeny poses rather limited demands on
866 exchange, especially compared to endopolygenic replication modes where the mother
867 cytoskeleton could pose a much larger barrier. An alternative role for the apical annuli is as a
868 gateway for a burst in dense granule secretion following completion of invasion (Carruthers and
869 Sibley, 1997): electron microscopy studies place dense granule release at this moment in an
870 apical location consistent with the position of the annuli (Dubremetz et al., 1993). Additional
871 studies on the role of the annuli during endopolygony are needed to firmly differentiate between
872 these two potential roles.

873 In conclusion, we define two principally different asexual cell division modes, external and
874 internal budding, which can both produce as few as two daughters per division round, but in
875 most situations produce many more daughters per division round. The bipartite centrosome
876 model and the identification of several regulators of cell cycle progression and checkpoints in
877 recent years provide a framework to explain these division modes, however the evolutionary
878 history and cell biological features defining, organizing and executing the various division
879 modes are much less clear. Expanding genetic and cell biological toolboxes for parasites
880 representing the various division modes provide exciting future avenues toward resolving the

Comparative apicomplexan cell division

881 exotic apicomplexan cell division modes and shedding light on the evolutionary pressures that
882 select for diversification and choices for different division modes at different developmental
883 stages.

884

885 **5 Conflict of Interest Statement**

886 The authors declare that the research was conducted in the absence of any commercial or
887 financial relationships that could be construed as a potential conflict of interest.

888

889 **6 Author Contributions Statement**

890 MG, HW, DH and MD conceived the experiments, HW performed the *C. suis* experiments, SD
891 and DH performed the *S. neurona* experiments, MG, CK, AP, BE, and CB performed the
892 *Babesia* experiments, KE and MG performed SIM microscopy, BE and IC performed electron
893 microscopy, MG wrote the manuscript and all authors edited the manuscript.

894

895 **7 Funding**

896 This study was supported by National Science Foundation (NSF) Major Research
897 Instrumentation grant 1626072, National Institute of Health grants AI110690 (MJG), AI110638
898 (MJG), AI128136 (MJG), AI144856 (MJG), and AI128480 (MTD), an American Heart
899 Association pre-doctoral fellowship 19PRE34380106 (CDK), a Profillinien start-up grant of the
900 University of Veterinary Medicine Vienna PP16110262 (HLW), an Australian NHMRC CJ
901 Martin fellowship (BE), a post-doctoral fellowship grant 17POST33670577 (KE), a Knights
902 Templar Eye Foundation Career Starter Award (KE), and USDA NIFA grant 2009-65109-05918
903 (DKH). The funders had no role in study design, data collection and analysis, decision to
904 publish, or preparation of the manuscript.

905

906 **8 Acknowledgements**

907 We thank Bret Judson and the Boston College Imaging Core as well as Stephan Handschuh and
908 the Imaging Core of the University of Veterinary Medicine Vienna for infrastructure and
909 support, Drs. Naomi Morrissette, Jaime Tarigo, and Jeff Dvorin for discussion, and Drs. David
910 Allred, Kirk Deitsch and Laura Kirkman for sharing reagents.

911

Comparative apicomplexan cell division

912 9 References

- 913
- 914 Al-Khattaf, F.S., Tremp, A.Z., and Dessens, J.T. (2015). Plasmodium alveolins possess distinct
915 but structurally and functionally related multi-repeat domains. *Parasitol Res* 114, 631-
916 639.
- 917 Alexandrov, A., Vignali, M., Lacount, D.J., Quartley, E., De Vries, C., De Rosa, D., Babulski, J.,
918 Mitchell, S.F., Schoenfeld, L.W., Fields, S., Hol, W.G., Dumont, M.E., Phizicky, E.M.,
919 and Grayhack, E.J. (2004). A facile method for high-throughput co-expression of protein
920 pairs. *Mol Cell Proteomics* 3, 934-938.
- 921 Alvarez, C.A., and Suvorova, E.S. (2017). Checkpoints of apicomplexan cell division identified
922 in *Toxoplasma gondii*. *PLoS Pathog* 13, e1006483.
- 923 Anderson-White, B.R., Beck, J.R., Chen, C.T., Meissner, M., Bradley, P.J., and Gubbels, M.J.
924 (2012). Cytoskeleton assembly in *Toxoplasma gondii* cell division. *Int. Rev. Cell Mol.*
925 *Biol.* 298, 1-31.
- 926 Anderson-White, B.R., Ivey, F.D., Cheng, K., Szatanek, T., Lorestani, A., Beckers, C.J.,
927 Ferguson, D.J., Sahoo, N., and Gubbels, M.J. (2011). A family of intermediate filament-
928 like proteins is sequentially assembled into the cytoskeleton of *Toxoplasma gondii*. *Cell*
929 *Microbiol* 13, 18-31.
- 930 Angrisano, F., Tan, Y.H., Sturm, A., Mcfadden, G.I., and Baum, J. (2012). Malaria parasite
931 colonisation of the mosquito midgut--placing the Plasmodium ookinete centre stage. *Int J*
932 *Parasitol* 42, 519-527.
- 933 Araki, T., Kawai, S., Kakuta, S., Kobayashi, H., Umeki, Y., Saito-Nakano, Y., Sasaki, T.,
934 Nagamune, K., Yasutomi, Y., Nozaki, T., Franke-Fayard, B., Khan, S.M., Hisaeda, H.,
935 and Annoura, T. (2019). Three-dimensional electron microscopy analysis reveals
936 endopolygeny-like nuclear architecture segregation in Plasmodium oocyst development.
937 *Parasitol Int* 76, 102034.
- 938 Arnot, D.E., Ronander, E., and Bengtsson, D.C. (2011). The progression of the intra-erythrocytic
939 cell cycle of Plasmodium falciparum and the role of the centriolar plaques in
940 asynchronous mitotic division during schizogony. *Int J Parasitol* 41, 71-80.
- 941 Barta, J.R., Martin, D.S., Carreno, R.A., Siddall, M.E., Profous-Juchelkat, H., Hozza, M.,
942 Powles, M.A., and Sundermann, C. (2001). Molecular phylogeny of the other tissue
943 coccidia: Lankesterella and Caryospora. *J Parasitol* 87, 121-127.
- 944 Bennink, S., Kiesow, M.J., and Pradel, G. (2016). The development of malaria parasites in the
945 mosquito midgut. *Cell Microbiol* 18, 905-918.
- 946 Berry, L., Chen, C.T., Francia, M.E., Guerin, A., Graindorge, A., Saliou, J.M., Grandmougin,
947 M., Wein, S., Bechara, C., Morlon-Guyot, J., Bordat, Y., Gubbels, M.J., Lebrun, M.,
948 Dubremetz, J.F., and Daher, W. (2018). *Toxoplasma gondii* chromosomal passenger
949 complex is essential for the organization of a functional mitotic spindle: a prerequisite for
950 productive endodyogeny. *Cell Mol Life Sci* 75, 4417-4443.
- 951 Berry, L., Chen, C.T., Reininger, L., Carvalho, T.G., El Hajj, H., Morlon-Guyot, J., Bordat, Y.,
952 Lebrun, M., Gubbels, M.J., Doerig, C., and Daher, W. (2016). The conserved
953 apicomplexan Aurora kinase TgArk3 is involved in endodyogeny, duplication rate and
954 parasite virulence. *Cell Microbiol* 18, 1106-1120.
- 955 Bock, R., Jackson, L., De Vos, A., and Jorgensen, W. (2004). Babesiosis of cattle. *Parasitology*
956 Suppl, S247-269.

Comparative apicomplexan cell division

- 957 Bornens, M., and Gonczy, P. (2014). Centrosomes back in the limelight. *Philos Trans R Soc*
958 *Lond B Biol Sci* 369.
- 959 Brooks, C.F., Francia, M.E., Gissot, M., Croken, M.M., Kim, K., and Striepen, B. (2011).
960 *Toxoplasma gondii* sequesters centromeres to a specific nuclear region throughout the
961 cell cycle. *Proc Natl Acad Sci U S A* 108, 3767-3772.
- 962 Brown, K.M., Suvorova, E., Farrell, A., Wiley, B.B., Marth, G., Gaffney, P.M., Gubbels, M.-J.,
963 White, M., and J., B.I. (2014). Forward Genetic Screening Identifies a Small Molecule
964 that Blocks *Toxoplasma gondii* Growth By Inhibiting Both Host- and Parasite-Encoded
965 Kinases. *PLoS Pathog* 10, e1004180.
- 966 Canning, E.U., and Sinden, R.E. (1973). The organization of the ookinete and observations on
967 nuclear division in oocysts of *Plasmodium berghei*. *Parasitology* 67, 29-40.
- 968 Carruthers, V.B., and Sibley, L.D. (1997). Sequential protein secretion from three distinct
969 organelles of *Toxoplasma gondii* accompanies invasion of human fibroblasts. *Eur J Cell*
970 *Biol* 73, 114-123.
- 971 Carter, V., Nacer, A.M., Underhill, A., Sinden, R.E., and Hurd, H. (2007). Minimum
972 requirements for ookinete to oocyst transformation in *Plasmodium*. *Int J Parasitol* 37,
973 1221-1232.
- 974 Carvalho, T.G., Doerig, C., and Reininger, L. (2013). Nima- and Aurora-related kinases of
975 malaria parasites. *Biochim Biophys Acta* 1834, 1336-1345.
- 976 Chakraborty, S., Roy, S., Mistry, H.U., Murthy, S., George, N., Bhandari, V., and Sharma, P.
977 (2017). Potential Sabotage of Host Cell Physiology by Apicomplexan Parasites for Their
978 Survival Benefits. *Front Immunol* 8, 1261.
- 979 Chen, A.L., Kim, E.W., Toh, J.Y., Vashisht, A.A., Rashoff, A.Q., Van, C., Huang, A.S., Moon,
980 A.S., Bell, H.N., Bentolila, L.A., Wohlschlegel, J.A., and Bradley, P.J. (2015a). Novel
981 components of the *Toxoplasma* inner membrane complex revealed by BioID. *MBio* 6,
982 e02357-02314.
- 983 Chen, A.L., Moon, A.S., Bell, H.N., Huang, A.S., Vashisht, A.A., Toh, J.Y., Lin, A.H.,
984 Nadipuram, S.M., Kim, E.W., Choi, C.P., Wohlschlegel, J.A., and Bradley, P.J. (2016).
985 Novel insights into the composition and function of the *Toxoplasma* IMC sutures. *Cell*
986 *Microbiol*.
- 987 Chen, C.T., and Gubbels, M.-J. (2019). TgCep250 is dynamically processed through the division
988 cycle and essential for structural integrity of the *Toxoplasma* centrosome. *Mol Biol Cell*
989 30, 1160-1169.
- 990 Chen, C.T., and Gubbels, M.J. (2013). The *Toxoplasma gondii* centrosome is the platform for
991 internal daughter budding as revealed by a Nek1 kinase mutant. *J Cell Sci* 126, 3344-
992 3355.
- 993 Chen, C.T., Kelly, M., Leon, J., Nwagbara, B., Ebbert, P., Ferguson, D.J., Lowery, L.A.,
994 Morrisette, N., and Gubbels, M.J. (2015b). Compartmentalized *Toxoplasma* EB1
995 bundles spindle microtubules to secure accurate chromosome segregation. *Mol Biol Cell*
996 26, 4562-4576.
- 997 Conrad, P.A., Denham, D., and Brown, C.G. (1986). Intraerythrocytic multiplication of *Theileria*
998 *parva* in vitro: an ultrastructural study. *Int J Parasitol* 16, 223-229.
- 999 Conrad, P.A., Kelly, B.G., and Brown, C.G. (1985). Intraerythrocytic schizogony of *Theileria*
1000 *annulata*. *Parasitology* 91 (Pt 1), 67-82.
- 1001 Conrad, P.A., Kjemtrup, A.M., Carreno, R.A., Thomford, J., Wainwright, K., Eberhard, M.,
1002 Quick, R., Telford, S.R., 3rd, and Herwaldt, B.L. (2006). Description of *Babesia duncani*

Comparative apicomplexan cell division

- 1003 n.sp. (Apicomplexa: Babesiidae) from humans and its differentiation from other
1004 piroplasms. *Int J Parasitol* 36, 779-789.
- 1005 Courjol, F., and Gissot, M. (2018). A coiled-coil protein is required for coordination of
1006 karyokinesis and cytokinesis in *Toxoplasma gondii*. *Cell Microbiol* 20, e12832.
- 1007 De Leon, J.C., Scheumann, N., Beatty, W., Beck, J.R., Tran, J.Q., Yau, C., Bradley, P.J., Gull,
1008 K., Wickstead, B., and Morrisette, N.S. (2013). A SAS-6-like protein suggests that the
1009 *Toxoplasma* conoid complex evolved from flagellar components. *Eukaryot Cell* 12,
1010 1009-1019.
- 1011 Dhara, A., and Sinai, A.P. (2016). A Cell Cycle-Regulated *Toxoplasma* Deubiquitinase,
1012 TgOTUD3A, Targets Polyubiquitins with Specific Lysine Linkages. *mSphere* 1.
- 1013 Dubey, J.P., Lindsay, D.S., Fritz, D., and Speer, C.A. (2001). Structure of *Sarcocystis* *neurona*
1014 *sarcocysts*. *J Parasitol* 87, 1323-1327.
- 1015 Dubey, R., Harrison, B., Dangoudoubyam, S., Bandini, G., Cheng, K., Kosber, A., Agop-
1016 Nersesian, C., Howe, D.K., Samuelson, J., Ferguson, D.J.P., and Gubbels, M.J. (2017).
1017 Differential Roles for Inner Membrane Complex Proteins across *Toxoplasma gondii* and
1018 *Sarcocystis* *neurona* Development. *mSphere* 2.
- 1019 Dubey, R., Staker, B.L., Foe, I.T., Bogyo, M., Myler, P.J., Ngo, H.M., and Gubbels, M.J. (2016).
1020 Membrane skeletal association and post-translational allosteric regulation of *Toxoplasma*
1021 *gondii* GAPDH1. *Mol Microbiol*.
- 1022 Dubremetz, J.F. (1971). L'ultrastructure du centriole et du centrocone chez la coccidie *Eimeria*
1023 *necatrix*. Étude au cours de la schizogonie. *J Microsc.* 23, 453-458.
- 1024 Dubremetz, J.F. (1973). [Ultrastructural study of schizogonic mitosis in the coccidian, *Eimeria*
1025 *necatrix* (Johnson 1930)]. *J Ultrastruct Res* 42, 354-376.
- 1026 Dubremetz, J.F. (1975). [Genesis of merozoites in the coccidia, *Eimeria necatrix*. Ultrastructural
1027 study]. *J Protozool* 22, 71-84.
- 1028 Dubremetz, J.F., Achbarou, A., Bermudes, D., and Joiner, K.A. (1993). Kinetics and pattern of
1029 organelle exocytosis during *Toxoplasma gondii*/host-cell interaction. *Parasitol Res* 79,
1030 402-408.
- 1031 Dubremetz, J.F., and Elsner, Y.Y. (1979). Ultrastructural study of schizogony of *Eimeria bovis*
1032 in cell cultures. *J Protozool* 26, 367-376.
- 1033 Engelberg, K., Chen, C.-T., Bechtel, T., Sánchez Guzmán, V., Drozda, A.A., Chavan, S.,
1034 Weerapana, E., and Gubbels, M.-J. (2019). The apical annuli of *Toxoplasma gondii* are
1035 composed of coiled-coil and signaling proteins embedded in the IMC sutures. *BioRxiv*
1036 doi.org/10.1101/711432
- 1037 Farrell, M., and Gubbels, M.J. (2014). The *Toxoplasma gondii* kinetochore is required for
1038 centrosome association with the centrocone (spindle pole). *Cellular Microbiology* 16, 78-
1039 94.
- 1040 Fawcett, D.W., Conrad, P.A., Grootenhuis, J.G., and Morzaria, S.P. (1987). Ultrastructure of the
1041 intra-erythrocytic stage of *Theileria* species from cattle and waterbuck. *Tissue Cell* 19,
1042 643-655.
- 1043 Ferguson, D.J., Birch-Andersen, A., Hutchison, W.M., and Siim, J.C. (1980). Ultrastructural
1044 observations on microgametogenesis and the structure of the microgamete of *Isospora*
1045 *felis*. *Acta Pathol Microbiol Scand [B]* 88, 151-159.
- 1046 Ferguson, D.J., Birch-Andersen, A., Siim, J.C., and Hutchison, W.M. (1979a). Ultrastructural
1047 studies on the sporulation of oocysts of *Toxoplasma gondii*. I. Development of the zygote

Comparative apicomplexan cell division

- 1048 and formation of the sporoblasts. *Acta pathologica et microbiologica Scandinavica*.
1049 *Section B, Microbiology* 87B, 171-181.
- 1050 Ferguson, D.J., Birch-Andersen, A., Siim, J.C., and Hutchison, W.M. (1979b). Ultrastructural
1051 studies on the sporulation of oocysts of *Toxoplasma gondii*. III. Formation of the
1052 sporozoites within the sporocysts. *Acta pathologica et microbiologica Scandinavica*.
1053 *Section B, Microbiology* 87, 253-260.
- 1054 Ferguson, D.J., Hutchison, W.M., Dunachie, J.F., and Siim, J.C. (1974). Ultrastructural study of
1055 early stages of asexual multiplication and microgametogony of *Toxoplasma gondii* in the
1056 small intestine of the cat. *Acta Pathol Microbiol Scand [B] Microbiol Immunol* 82, 167-
1057 181.
- 1058 Ferguson, D.J., Sahoo, N., Pinches, R.A., Bumstead, J.M., Tomley, F.M., and Gubbels, M.J.
1059 (2008). MORN1 has a conserved role in asexual and sexual development across the
1060 Apicomplexa. *Eukaryot Cell* 7, 698-711.
- 1061 Francia, M.E., Dubremetz, J.F., and Morrissette, N.S. (2015). Basal body structure and
1062 composition in the apicomplexans *Toxoplasma* and *Plasmodium*. *Cilia* 5, 3.
- 1063 Francia, M.E., Jordan, C.N., Patel, J.D., Sheiner, L., Demerly, J.L., Fellows, J.D., De Leon, J.C.,
1064 Morrissette, N.S., Dubremetz, J.F., and Striepen, B. (2012). Cell division in
1065 Apicomplexan parasites is organized by a homolog of the striated rootlet fiber of algal
1066 flagella. *PLoS biology* 10, e1001444.
- 1067 Francia, M.E., and Striepen, B. (2014). Cell division in apicomplexan parasites. *Nature reviews*.
1068 *Microbiology* 12, 125-136.
- 1069 Frenal, K., Dubremetz, J.F., Lebrun, M., and Soldati-Favre, D. (2017a). Gliding motility powers
1070 invasion and egress in Apicomplexa. *Nat Rev Microbiol* 15, 645-660.
- 1071 Frenal, K., Jacot, D., Hammoudi, P.M., Graindorge, A., Maco, B., and Soldati-Favre, D. (2017b).
1072 Myosin-dependent cell-cell communication controls synchronicity of division in acute
1073 and chronic stages of *Toxoplasma gondii*. *Nat Commun* 8, 15710.
- 1074 Frenal, K., Marq, J.B., Jacot, D., Polonais, V., and Soldati-Favre, D. (2014). Plasticity between
1075 MyoC- and MyoA-glideosomes: an example of functional compensation in *Toxoplasma*
1076 *gondii* invasion. *PLoS Pathog* 10, e1004504.
- 1077 Friedhoff, K.T., and Scholtyseck, E. (1977). Fine structural identification of erythrocytic stages
1078 of *Babesia bigemina*, *Babesia divergens* and *Babesia ovis*. *Protistologica* 13, 195-204.
- 1079 Fung, C., Beck, J.R., Robertson, S.D., Gubbels, M.J., and Bradley, P.J. (2012). *Toxoplasma* ISP4
1080 is a central IMC sub-compartment protein whose localization depends on palmitoylation
1081 but not myristoylation. *Mol Biochem Parasitol* 184, 99-108.
- 1082 Gaji, R.Y., Behnke, M.S., Lehmann, M.M., White, M.W., and Carruthers, V.B. (2011). Cell
1083 cycle-dependent, intercellular transmission of *Toxoplasma gondii* is accompanied by
1084 marked changes in parasite gene expression. *Mol Microbiol* 79, 192-204.
- 1085 Ganter, M., Goldberg, J.M., Dvorin, J.D., Paulo, J.A., King, J.G., Tripathi, A.K., Paul, A.S.,
1086 Yang, J., Coppens, I., Jiang, R.H., Elsworth, B., Baker, D.A., Dinglasan, R.R., Gygi, S.P.,
1087 and Duraisingh, M.T. (2017). *Plasmodium falciparum* CRK4 directs continuous rounds
1088 of DNA replication during schizogony. *Nat Microbiol* 2, 17017.
- 1089 Gardiner, C.H., Fayer, R., and Dubey, J.P. (1998). *An Atlas of Protozoan Parasites in Animal*
1090 *Tissues*. Armed Forces Institute of Pathology.
- 1091 Gaskins, E., Gilk, S., Devore, N., Mann, T., Ward, G., and Beckers, C. (2004). Identification of
1092 the membrane receptor of a class XIV myosin in *Toxoplasma gondii*. *J Cell Biol* 165,
1093 383-393.

Comparative apicomplexan cell division

- 1094 Gerald, N., Mahajan, B., and Kumar, S. (2011). Mitosis in the human malaria parasite
1095 *Plasmodium falciparum*. *Eukaryot Cell* 10, 474-482.
- 1096 Goldman, M., Carver, R.K., and Sulzer, A.J. (1958). Reproduction of *Toxoplasma gondii* by
1097 internal budding. *J Parasitol* 44, 161-171.
- 1098 Goodenough, U., Roth, R., Kariyawasam, T., He, A., and Lee, J.H. (2018). Epiplasts: Membrane
1099 Skeletons and Epiplastin Proteins in Euglenids, Glaucophytes, Cryptophytes, Ciliates,
1100 Dinoflagellates, and Apicomplexans. *MBio* 9.
- 1101 Gould, S.B., Tham, W.H., Cowman, A.F., Mcfadden, G.I., and Waller, R.F. (2008). Alveolins, a
1102 new family of cortical proteins that define the protist infrakingdom Alveolata. *Mol Biol*
1103 *Evol* 25, 1219-1230.
- 1104 Gruring, C., Heiber, A., Kruse, F., Ungefehr, J., Gilberger, T.W., and Spielmann, T. (2011).
1105 Development and host cell modifications of *Plasmodium falciparum* blood stages in four
1106 dimensions. *Nat Commun* 2, 165.
- 1107 Gubbels, M.J., and Duraisingh, M.T. (2012). Evolution of apicomplexan secretory organelles. *Int*
1108 *J Parasitol* 42, 1071-1081.
- 1109 Gubbels, M.J., Vaishnava, S., Boot, N., Dubremetz, J.F., and Striepen, B. (2006). A MORN-
1110 repeat protein is a dynamic component of the *Toxoplasma gondii* cell division apparatus.
1111 *J Cell Sci* 119, 2236-2245.
- 1112 Gubbels, M.J., Wieffer, M., and Striepen, B. (2004). Fluorescent protein tagging in *Toxoplasma*
1113 *gondii*: identification of a novel inner membrane complex component conserved among
1114 Apicomplexa. *Mol Biochem Parasitol* 137, 99-110.
- 1115 Hammond, D.M. (1973). *The Coccidia: Eimeria, Isospora, Toxoplasma, and related genera*.
1116 University Park Press.
- 1117 Heaslip, A.T., Dzierszynski, F., Stein, B., and Hu, K. (2010). TgMORN1 Is a Key Organizer for
1118 the Basal Complex of *Toxoplasma gondii*. *PLoS Pathog* 6, e1000754.
- 1119 Hepler, P.K., Huff, C.G., and Sprinz, H. (1966). The fine structure of the exoerythrocytic stages
1120 of *Plasmodium fallax*. *J Cell Biol* 30, 333-358.
- 1121 Hoeijmakers, W.A., Flueck, C., Francoijs, K.J., Smits, A.H., Wetzel, J., Volz, J.C., Cowman,
1122 A.F., Voss, T., Stunnenberg, H.G., and Bartfai, R. (2012). *Plasmodium falciparum*
1123 centromeres display a unique epigenetic makeup and cluster prior to and during
1124 schizogony. *Cell Microbiol* 14, 1391-1401.
- 1125 Howe, D.K., Yeargan, M., Simpson, L., and Dangoudoubiyam, S. (2018). Molecular Genetic
1126 Manipulation of *Sarcocystis neurona*. *Curr Protoc Microbiol* 48, 20D 22 21-20D 22 14.
- 1127 Howells, R.E., and Davies, E.E. (1971a). Nuclear division in the oocyst of *Plasmodium berghei*.
1128 *Ann Trop Med Parasitol* 65, 451-459.
- 1129 Howells, R.E., and Davies, E.E. (1971b). Post-meiotic nuclear divisions in the oocyst of
1130 *Plasmodium berghei*. *Trans R Soc Trop Med Hyg* 65, 421.
- 1131 Hu, K. (2008). Organizational changes of the daughter basal complex during the parasite
1132 replication of *Toxoplasma gondii*. *PLoS Pathog* 4, e10.
- 1133 Hu, K., Johnson, J., Florens, L., Fraunholz, M., Suravajjala, S., Dilullo, C., Yates, J., Roos, D.S.,
1134 and Murray, J.M. (2006). Cytoskeletal components of an invasion machine--the apical
1135 complex of *Toxoplasma gondii*. *PLoS Pathog* 2, e13.
- 1136 Hu, K., Roos, D.S., Angel, S.O., and Murray, J.M. (2004). Variability and heritability of cell
1137 division pathways in *Toxoplasma gondii*. *J Cell Sci* 117, 5697-5705.
- 1138 Jakel, T., Wallstein, E., Muncheberg, F., Archer-Baumann, C., Weingarten, B., Kliemt, D., and
1139 Mackenstedt, U. (2001). Binding of a monoclonal antibody to sporozoites of *Sarcocystis*

Comparative apicomplexan cell division

- 1140 singaporensis enhances escape from the parasitophorous vacuole, which is necessary for
1141 intracellular development. *Infect Immun* 69, 6475-6482.
- 1142 Jalovecka, M., Hajdusek, O., Sojka, D., Kopacek, P., and Malandrin, L. (2018). The Complexity
1143 of Piroplasms Life Cycles. *Front Cell Infect Microbiol* 8, 248.
- 1144 Jayabalasingham, B., Bano, N., and Coppens, I. (2010). Metamorphosis of the malaria parasite in
1145 the liver is associated with organelle clearance. *Cell Res* 20, 1043-1059.
- 1146 Jerka-Dziadosz, M., and Frankel, J. (1995). The effects of lithium chloride on pattern formation
1147 in *Tetrahymena thermophila*. *Dev Biol* 171, 497-506.
- 1148 Jerka-Dziadosz, M., Jenkins, L.M., Nelsen, E.M., Williams, N.E., Jaeckel-Williams, R., and
1149 Frankel, J. (1995). Cellular polarity in ciliates: persistence of global polarity in a
1150 disorganized mutant of *Tetrahymena thermophila* that disrupts cytoskeletal organization.
1151 *Dev Biol* 169, 644-661.
- 1152 Joyner, L.P., and Long, P.L. (1974). The specific characters of the *Eimeria*, with special
1153 reference to the coccidia of the fowl. *Avian Pathol* 3, 145-157.
- 1154 Kono, M., Heincke, D., Wilcke, L., Wong, T., Bruns, C., Herrmann, S., Spielmann, T., and
1155 Gilberger, T.W. (2016). Pellicle formation in the malaria parasite. *J Cell Sci*.
- 1156 Kono, M., Herrmann, S., Loughran, N.B., Cabrera, A., Engelberg, K., Lehmann, C., Sinha, D.,
1157 Prinz, B., Ruch, U., Heussler, V., Spielmann, T., Parkinson, J., and Gilberger, T.W.
1158 (2012). Evolution and Architecture of the Inner Membrane Complex in Asexual and
1159 Sexual Stages of the Malaria Parasite. *Molecular biology and evolution* 29, 2113-2132.
- 1160 Kvicerova, J., and Hypsa, V. (2013). Host-parasite incongruences in rodent *Eimeria* suggest
1161 significant role of adaptation rather than cophylogeny in maintenance of host specificity.
1162 *PLoS One* 8, e63601.
- 1163 Le Roch, K., Sestier, C., Dorin, D., Waters, N., Kappes, B., Chakrabarti, D., Meijer, L., and
1164 Doerig, C. (2000). Activation of a *Plasmodium falciparum* cdc2-related kinase by
1165 heterologous p25 and cyclin H. Functional characterization of a *P. falciparum* cyclin
1166 homologue. *J Biol Chem* 275, 8952-8958.
- 1167 Leander, B.S., and Keeling, P.J. (2003). Morphostasis in alveolate evolution. *trends in Ecology*
1168 *and Evolution* 18, 395-402.
- 1169 Lehtreck, K.F. (2003). Striated fiber assemblin in apicomplexan parasites. *Mol Biochem*
1170 *Parasitol* 128, 95-99.
- 1171 Lentini, G., Dubois, D.J., Maco, B., Soldati-Favre, D., and Frenal, K. (2019). The roles of
1172 Centrin 2 and Dynein Light Chain 8a in apical secretory organelles discharge of
1173 *Toxoplasma gondii*. *Traffic*.
- 1174 Lindsay, D.S., Stuart, B.P., Wheat, B.E., and Ernst, J.V. (1980). Endogenous development of the
1175 swine coccidium, *Isospora suis* Biester 1934. *J Parasitol* 66, 771-779.
- 1176 Lorestani, A., Ivey, F.D., Thirugnanam, S., Busby, M.A., Marth, G.T., Cheeseman, I.M., and
1177 Gubbels, M.J. (2012). Targeted proteomic dissection of *Toxoplasma* cytoskeleton sub-
1178 compartments using MORN1. *Cytoskeleton* 69, 1069-1085.
- 1179 Lorestani, A., Sheiner, L., Yang, K., Robertson, S.D., Sahoo, N., Brooks, C.F., Ferguson, D.J.,
1180 Striepen, B., and Gubbels, M.J. (2010). A *Toxoplasma* MORN1 Null Mutant Undergoes
1181 Repeated Divisions but Is Defective in Basal Assembly, Apicoplast Division and
1182 Cytokinesis. *PLoS ONE* 5, e12302.
- 1183 Luder, C.G., Stanway, R.R., Chaussepied, M., Langsley, G., and Heussler, V.T. (2009).
1184 Intracellular survival of apicomplexan parasites and host cell modification. *Int J Parasitol*
1185 39, 163-173.

Comparative apicomplexan cell division

- 1186 Mahajan, B., Selvapandiyan, A., Gerald, N.J., Majam, V., Zheng, H., Wickramarachchi, T.,
1187 Tiwari, J., Fujioka, H., Moch, J.K., Kumar, N., Aravind, L., Nakhasi, H.L., and Kumar,
1188 S. (2008). Centrins, cell cycle regulation proteins in human malaria parasite *Plasmodium*
1189 *falciparum*. *J Biol Chem* 283, 31871-31883.
- 1190 Mann, T., Gaskins, E., and Beckers, C. (2002). Proteolytic Processing of TgIMC1 during
1191 Maturation of the Membrane Skeleton of *Toxoplasma gondii*. *J Biol Chem* 277, 41240-
1192 41246.
- 1193 Martorelli Di Genova, B., Wilson, S.K., Dubey, J.P., and Knoll, L.J. (2019). Intestinal delta-6-
1194 desaturase activity determines host range for *Toxoplasma* sexual reproduction. *PLoS Biol*
1195 17, e3000364.
- 1196 Matthews, H., Duffy, C.W., and Merrick, C.J. (2018). Checks and balances? DNA replication
1197 and the cell cycle in *Plasmodium*. *Parasit Vectors* 11, 216.
- 1198 Matuschka, F.R., and Heydorn, A.O. (1980). "Die Entwicklung von *Isospora suis* Biester und
1199 Murray 1934 (Sporozoa : Coccidia : Eimeriidae) im Schwein," in *Zoologische Beiträge*,
1200 ed. K. Herter. (Berlin: Duncker & Humblot), 405-476.
- 1201 Mecklenburg, K.L. (2007). *Drosophila* retinophilin contains MORN repeats and is conserved in
1202 humans. *Mol Genet Genomics* 277, 481-489.
- 1203 Mehlhorn, H., and Shein, E. (1984). The piroplasms: life cycle and sexual stages. *Adv Parasitol*
1204 23, 37-103.
- 1205 Merckx, A., Le Roch, K., Nivez, M.P., Dorin, D., Alano, P., Gutierrez, G.J., Nebreda, A.R.,
1206 Goldring, D., Whittle, C., Patterson, S., Chakrabarti, D., and Doerig, C. (2003).
1207 Identification and initial characterization of three novel cyclin-related proteins of the
1208 human malaria parasite *Plasmodium falciparum*. *J Biol Chem* 278, 39839-39850.
- 1209 Moltmann, U.G., Mehlhorn, H., and Friedhoff, K.T. (1982). Ultrastructural study of the
1210 development of *Babesia ovis* (Piroplasmia) in the ovary of the vector tick *Rhipicephalus*
1211 *bursa*. *J Protozool* 29, 30-38.
- 1212 Moltmann, U.G., Mehlhorn, H., Schein, E., Voigt, W.P., and Friedhoff, K.T. (1983).
1213 Ultrastructural study on the development of *Babesia equi* (Coccidia: Piroplasmia) in the
1214 salivary glands of its vector ticks. *J Protozool* 30, 218-225.
- 1215 Morlon-Guyot, J., Francia, M.E., Dubremetz, J.F., and Daher, W. (2017). Towards a molecular
1216 architecture of the centrosome in *Toxoplasma gondii*. *Cytoskeleton (Hoboken)* 74, 55-71.
- 1217 Morriswood, B., and Schmidt, K. (2015). A MORN Repeat Protein Facilitates Protein Entry into
1218 the Flagellar Pocket of *Trypanosoma brucei*. *Eukaryot Cell* 14, 1081-1093.
- 1219 Naumov, A., Kratzer, S., Ting, L.M., Kim, K., Suvorova, E.S., and White, M.W. (2017). The
1220 *Toxoplasma* Centrocone Houses Cell Cycle Regulatory Factors. *MBio* 8.
- 1221 Nishi, M., Hu, K., Murray, J.M., and Roos, D.S. (2008). Organellar dynamics during the cell
1222 cycle of *Toxoplasma gondii*. *J Cell Sci* 121, 1559-1568.
- 1223 Nishikawa, Y., Quittnat, F., Stedman, T.T., Voelker, D.R., Choi, J.Y., Zahn, M., Yang, M.,
1224 Pypaert, M., Joiner, K.A., and Coppens, I. (2005). Host cell lipids control cholesteryl
1225 ester synthesis and storage in intracellular *Toxoplasma*. *Cell Microbiol* 7, 849-867.
- 1226 Ouologuem, D.T., and Roos, D.S. (2014). Dynamics of the *Toxoplasma gondii* inner membrane
1227 complex. *J Cell Sci* 127, 3320-3330.
- 1228 Pandey, R., Zeeshan, M., Ferguson, D.J.P., Markus, R., Brady, D., Daniel, E., Stanway, R.R.,
1229 Holder, A.A., Guttery, D.S., and Tewari, R. (2019). Real-time dynamics of *Plasmodium*
1230 NDC80 as a marker for the kinetochore during atypical mitosis and meiosis. *bioRxiv*
1231 <http://dx.doi.org/10.1101/767830>.

Comparative apicomplexan cell division

- 1232 Paul, A.S., Moreira, C.K., Elsworth, B., Allred, D.R., and Duraisingh, M.T. (2016). Extensive
1233 Shared Chemosensitivity between Malaria and Babesiosis Blood-Stage Parasites.
1234 *Antimicrob Agents Chemother* 60, 5059-5063.
- 1235 Periz, J., Del Rosario, M., Mcstea, A., Gras, S., Loney, C., Wang, L., Martin-Fernandez, M.L.,
1236 and Meissner, M. (2019). A highly dynamic F-actin network regulates transport and
1237 recycling of micronemes in *Toxoplasma gondii* vacuoles. *Nat Commun* 10, 4183.
- 1238 Periz, J., Whitelaw, J., Harding, C., Gras, S., Del Rosario Minina, M.I., Latorre-Barragan, F.,
1239 Lemgruber, L., Reimer, M.A., Insall, R., Heaslip, A., and Meissner, M. (2017).
1240 *Toxoplasma gondii* F-actin forms an extensive filamentous network required for material
1241 exchange and parasite maturation. *Elife* 6.
- 1242 Potgieter, F.T., and Els, H.J. (1976). Light and electron microscopic observations on the
1243 development of small merozoites of *Babesia bovis* in *Boophilus microplus* larvae.
1244 *Onderstepoort J Vet Res* 43, 123-128.
- 1245 Potgieter, F.T., and Els, H.J. (1977). The fine structure of intra-erythrocytic stages of *Babesia*
1246 *bigemina*. *Onderstepoort J Vet Res* 44, 157-168.
- 1247 Reed, S.M., Furr, M., Howe, D.K., Johnson, A.L., Mackay, R.J., Morrow, J.K., Pusterla, N., and
1248 Witonsky, S. (2016). Equine Protozoal Myeloencephalitis: An Updated Consensus
1249 Statement with a Focus on Parasite Biology, Diagnosis, Treatment, and Prevention. *J Vet*
1250 *Intern Med* 30, 491-502.
- 1251 Reilly, H.B., Wang, H., Steuter, J.A., Marx, A.M., and Ferdig, M.T. (2007). Quantitative
1252 dissection of clone-specific growth rates in cultured malaria parasites. *Int J Parasitol* 37,
1253 1599-1607.
- 1254 Reininger, L., Wilkes, J.M., Bourgade, H., Miranda-Saavedra, D., and Doerig, C. (2011). An
1255 essential Aurora-related kinase transiently associates with spindle pole bodies during
1256 *Plasmodium falciparum* erythrocytic schizogony. *Mol Microbiol* 79, 205-221.
- 1257 Robbins, J.A., Absalon, S., Streva, V.A., and Dvorin, J.D. (2017). The Malaria Parasite Cyclin H
1258 Homolog PfCyc1 Is Required for Efficient Cytokinesis in Blood-Stage *Plasmodium*
1259 *falciparum*. *MBio* 8.
- 1260 Roberts, R., Lister, I., Schmitz, S., Walker, M., Veigel, C., Trinick, J., Buss, F., and Kendrick-
1261 Jones, J. (2004). Myosin VI: cellular functions and motor properties. *Philosophical*
1262 *transactions of the Royal Society of London. Series B, Biological sciences* 359, 1931-
1263 1944.
- 1264 Roberts, W.L., Hammond, D.M., Anderson, L.C., and Speer, C.A. (1970). Ultrastructural study
1265 of schizogony in *Eimeria callospermophili*. *J Protozool* 17, 584-592.
- 1266 Roques, M., Stanway, R.R., Rea, E.I., Markus, R., Brady, D., Holder, A.A., Guttery, D.S., and
1267 Tewari, R. (2019). *Plasmodium* centrin PbCEN-4 localizes to the putative MTOC and is
1268 dispensable for malaria parasite proliferation. *Biol Open* 8.
- 1269 Roques, M., Wall, R.J., Douglass, A.P., Ramaprasad, A., Ferguson, D.J., Kaindama, M.L.,
1270 Brusini, L., Joshi, N., Rchiad, Z., Brady, D., Guttery, D.S., Wheatley, S.P., Yamano, H.,
1271 Holder, A.A., Pain, A., Wickstead, B., and Tewari, R. (2015). *Plasmodium* P-Type
1272 Cyclin CYC3 Modulates Endomitotic Growth during Oocyst Development in
1273 Mosquitoes. *PLoS Pathog* 11, e1005273.
- 1274 Rosenthal, B.M., Dunams-Morel, D., Ostoros, G., and Molnar, K. (2016). Coccidian parasites of
1275 fish encompass profound phylogenetic diversity and gave rise to each of the major
1276 parasitic groups in terrestrial vertebrates. *Infect Genet Evol* 40, 219-227.

Comparative apicomplexan cell division

- 1277 Rudlaff, R.M., Kraemer, S., Streva, V.A., and Dvorin, J.D. (2019). An essential contractile ring
1278 protein controls cell division in *Plasmodium falciparum*. *Nat Commun* 10, 2181.
- 1279 Rudzinska, M.A. (1981). "Morphologic aspects of host-cell-parasite relationships in babesiosis,"
1280 in *Babesiosis*, eds. M. Ristic & J.P. Kreier. (New York, NY: Academic Press), 87–142.
- 1281 Samad, N., Hliscs, M., Katris, N.J., Mcfadden, G.I., and Waller, R.F. (2015). Microtubule
1282 associated protein SPM3 shows dynamic repositioning during cytokinesis and is required
1283 for nascent daughter formation. *13th International Congress on Toxoplasmosis &*
1284 *Toxoplasma gondii Biology, At Gettysburg College, in Gettysburg PA (USA)*
1285 <http://hdl.handle.net/11343/194103>, 190.
- 1286 Schein, E., Mehlhorn, H., and Voigt, W.P. (1979). Electron microscopical studies on the
1287 development of *Babesia canis* (Sporozoa) in the salivary glands of the vector tick
1288 *Dermacentor reticulatus*. *Acta Trop* 36, 229-241.
- 1289 Scholtyseck, E. (1979). *Fine Structure of Parasitic Protozoa*. Springer.
- 1290 Schrevel, J., Asfaux-Foucher, G., and Bafort, J.M. (1977). [Ultrastructural study of multiple
1291 mitoses during sporogony of *Plasmodium b. berghei*]. *J Ultrastruct Res* 59, 332-350.
- 1292 Sharma, P., and Chitnis, C.E. (2013). Key molecular events during host cell invasion by
1293 Apicomplexan pathogens. *Curr Opin Microbiol* 16, 432-437.
- 1294 Shaw, M.K., and Tilney, L.G. (1992). How individual cells develop from a syncytium:
1295 merogony in *Theileria parva* (Apicomplexa). *J Cell Sci* 101 (Pt 1), 109-123.
- 1296 Sheffield, H.G., and Melton, M.L. (1968). The fine structure and reproduction of *Toxoplasma*
1297 *gondii*. *J Parasitol* 54, 209-226.
- 1298 Shetty, J., Klotz, K.L., Wolkowicz, M.J., Flickinger, C.J., and Herr, J.C. (2007). Radial spoke
1299 protein 44 (human meichoacidin) is an axonemal alloantigen of sperm and cilia. *Gene*
1300 396, 93-107.
- 1301 Shrestha, A., Abd-Elfattah, A., Freudenschuss, B., Hinney, B., Palmieri, N., Ruttkowski, B., and
1302 Joachim, A. (2015). *Cystoisospora suis* - A Model of Mammalian Cystoisosporosis.
1303 *Front Vet Sci* 2, 68.
- 1304 Sievers, F., Wilm, A., Dineen, D., Gibson, T.J., Karplus, K., Li, W., Lopez, R., McWilliam, H.,
1305 Remmert, M., Soding, J., Thompson, J.D., and Higgins, D.G. (2011). Fast, scalable
1306 generation of high-quality protein multiple sequence alignments using Clustal Omega.
1307 *Mol Syst Biol* 7, 539.
- 1308 Silmon De Monerri, N.C., Yakubu, R.R., Chen, A.L., Bradley, P.J., Nieves, E., Weiss, L.M., and
1309 Kim, K. (2015). The Ubiquitin Proteome of *Toxoplasma gondii* Reveals Roles for Protein
1310 Ubiquitination in Cell-Cycle Transitions. *Cell Host Microbe* 18, 621-633.
- 1311 Simonetti, A.B. (1996). The biology of malarial parasite in the mosquito--a review. *Mem Inst*
1312 *Oswaldo Cruz* 91, 519-541.
- 1313 Sinden, R.E. (1983). Sexual development of malarial parasites. *Adv Parasitol* 22, 153-216.
- 1314 Sinden, R.E., Canning, E.U., Bray, R.S., and Smalley, M.E. (1978). Gametocyte and gamete
1315 development in *Plasmodium falciparum*. *Proc R Soc Lond B Biol Sci* 201, 375-399.
- 1316 Sinden, R.E., and Strong, K. (1978). An ultrastructural study of the sporogonic development of
1317 *Plasmodium falciparum* in *Anopheles gambiae*. *Trans R Soc Trop Med Hyg* 72, 477-491.
- 1318 Spreng, B., Fleckenstein, H., Kubler, P., Di Biagio, C., Benz, M., Patra, P., Schwarz, U.S.,
1319 Cyrklaff, M., and Frischknecht, F. (2019). Microtubule number and length determine
1320 cellular shape and function in *Plasmodium*. *EMBO J* 38, e100984.

Comparative apicomplexan cell division

- 1321 Stanway, R.R., Mueller, N., Zobiak, B., Graewe, S., Froehlke, U., Zessin, P.J., Aepfelbacher, M.,
1322 and Heussler, V.T. (2011). Organelle segregation into Plasmodium liver stage
1323 merozoites. *Cell Microbiol* 13, 1768-1782.
- 1324 Stuart, B.P., Bedell, D.M., and Lindsay, D.S. (1982). Coccidiosis in swine: a search for
1325 extraintestinal stages of *Isospora suis*. *Vet Rec* 110, 82-83.
- 1326 Suarez, C.E., Alzan, H.F., Silva, M.G., Rathinasamy, V., Poole, W.A., and Cooke, B.M. (2019).
1327 Unravelling the cellular and molecular pathogenesis of bovine babesiosis: is the sky the
1328 limit? *Int J Parasitol* 49, 183-197.
- 1329 Sugi, T., Kawazu, S., Horimoto, T., and Kato, K. (2015). A single mutation in the gatekeeper
1330 residue in TgMAPKL-1 restores the inhibitory effect of a bumped kinase inhibitor on the
1331 cell cycle. *Int J Parasitol Drugs Drug Resist* 5, 1-8.
- 1332 Suvorova, E.S., Francia, M., Striepen, B., and White, M.W. (2015). A novel bipartite centrosome
1333 coordinates the apicomplexan cell cycle. *PLoS Biol* 13, e1002093.
- 1334 Tokuhiro, K., Hirose, M., Miyagawa, Y., Tsujimura, A., Irie, S., Isotani, A., Okabe, M., Toyama,
1335 Y., Ito, C., Toshimori, K., Takeda, K., Oshio, S., Tainaka, H., Tsuchida, J., Okuyama, A.,
1336 Nishimune, Y., and Tanaka, H. (2008). Meichroacidin containing the MORN motif is
1337 essential for spermatozoa morphogenesis. *J Biol Chem*.
- 1338 Trojan, P., Krauss, N., Choe, H.W., Giessl, A., Pulvermuller, A., and Wolfrum, U. (2008).
1339 Centrioles in retinal photoreceptor cells: regulators in the connecting cilium. *Prog Retin*
1340 *Eye Res* 27, 237-259.
- 1341 Uilenberg, G. (2006). Babesia--a historical overview. *Vet Parasitol* 138, 3-10.
- 1342 Vaishnava, S., Morrison, D.P., Gaji, R.Y., Murray, J.M., Entzeroth, R., Howe, D.K., and
1343 Striepen, B. (2005). Plastid segregation and cell division in the apicomplexan parasite
1344 *Sarcocystis neurona*. *J Cell Sci* 118, 3397-3407.
- 1345 Vaughan, A.M., and Kappe, S.H.I. (2017). Malaria Parasite Liver Infection and Exoerythrocytic
1346 Biology. *Cold Spring Harb Perspect Med* 7.
- 1347 Vega, C.A., Buening, G.M., Green, T.J., and Carson, C.A. (1985). In vitro cultivation of *Babesia*
1348 *bigemina*. *Am J Vet Res* 46, 416-420.
- 1349 Wall, R.J., Roques, M., Katris, N.J., Koreny, L., Stanway, R.R., Brady, D., Waller, R.F., and
1350 Tewari, R. (2016). SAS6-like protein in Plasmodium indicates that conoid-associated
1351 apical complex proteins persist in invasive stages within the mosquito vector. *Sci Rep* 6,
1352 28604.
- 1353 Warrenfeltz, S., Basenko, E.Y., Crouch, K., Harb, O.S., Kissinger, J.C., Roos, D.S.,
1354 Shanmugasundram, A., and Silva-Franco, F. (2018). EuPathDB: The Eukaryotic
1355 Pathogen Genomics Database Resource. *Methods Mol Biol* 1757, 69-113.
- 1356 Watts, E., Zhao, Y., Dhara, A., Eller, B., Patwardhan, A., and Sinai, A.P. (2015). Novel
1357 Approaches Reveal that *Toxoplasma gondii* Bradyzoites within Tissue Cysts Are
1358 Dynamic and Replicating Entities In Vivo. *MBio* 6, e01155-01115.
- 1359 White, M.W., and Suvorova, E.S. (2018). Apicomplexa Cell Cycles: Something Old, Borrowed,
1360 Lost, and New. *Trends Parasitol* 34, 759-771.
- 1361 Worliczek, H.L., Rutkowski, B., Schwarz, L., Witter, K., Tschulenk, W., and Joachim, A.
1362 (2013). *Isospora suis* in an epithelial cell culture system - an in vitro model for sexual
1363 development in coccidia. *PLoS One* 8, e69797.
- 1364
- 1365

Comparative apicomplexan cell division

1366 Legend to Figures

1367

1368 **Figure 1. Select apicomplexan phylogeny and division modes.** 18S ribosomal RNA based
1369 phylogeny of species whose division modes have been studied. *Cryptosporidium* spp. were used
1370 as outgroup. Bars on the right indicate different naming and biological relationships, with
1371 asexual division modes in blue and red. “in vacuole” and “in cytoplasm” indicate whether
1372 asexual replication occurs in a parasitophorous vacuole, or whether the parasite escapes from the
1373 vacuole and resides in the cytoplasm of the host cell for its replication. Note that only the acute
1374 stage merozoites of *S. neurona* replicates by endopolygeny in the cytoplasm, whereas merozoites
1375 preceding the bradyzoites as well as the bradyzoites divide by endodyogeny within a vacuole
1376 supporting a proteoglycan cyst wall. Furthermore, tissue cysts for *C. suis* have not been
1377 described and this lacking ability is likely a secondary loss. In addition, for several *Plasmodium*
1378 spp. (Simonetti, 1996), as well as *Babesia* and *Theileria* spp. (Jalovecka et al., 2018) it has been
1379 shown that sporozoite formation progresses without karyokinesis to produce large polyploid
1380 nuclei while budding is from the cortex. We note that *Plasmodium* sporozoites infect hepatocytes
1381 wherein they divide by schizogony and manipulate the hepatocytes to expand their size, whereas
1382 *Theileria* sporozoites infect white blood cells, replicate by schizogony (Shaw and Tilney, 1992)
1383 and trigger white blood expansion as well as division (i.e. transformation, which basically is
1384 leukemia (Luder et al., 2009; Chakraborty et al., 2017), which contrasts with *Babesia* sporozoites
1385 as they directly infect red blood cells. “epg with kk” means “endopolygeny with karyokinesis”,
1386 in case of *E. callospermophili*; “k.a.” means “kinete amplification”, in case of select *Babesia* spp.
1387

1388 **Figure 2. Apicomplexan asexual cell division by schizogony. A.** Schematic representation of
1389 progressive cell division steps during ‘classic’ schizogony. The mother’s cytoskeleton (present in
1390 1) is disassembled following successful host cell invasion resulting in a pleomorphic cell (2)
1391 before onset of mitosis and karyokinesis, which can be asynchronous (3). Daughter cells bud
1392 from the cortex (4/5), positioned by the centrosome anchored at the plasma membrane (4). **B.**
1393 Schematic representation of phases in the cell division during schizogony with limited
1394 karyokinesis as seen during Hemosporidian sporogony. Karyokinesis is inconsistently
1395 following each S/M-phase leading to a nuclei population with varying levels of ploidity. Note
1396 that nuclear cycles within the same nucleoplasm are similar (1), whereas budding is synchronous

Comparative apicomplexan cell division

1397 for all nuclei and linked to a final round of S/M (2). Note that the number of offspring in both
1398 forms of schizogony can reach into the 1000s, which is not represented in the schematics.
1399 Chromosome condensation does not occur and the chromosomes are only drawn to convey the
1400 principle of spindle pole attachment. Mother cytoplasm represented in grey, daughter cytoplasm
1401 in pink.

1402

1403 **Figure 3. Binary fission by *Babesia* spp. A-D. *Babesia bigemina* iRBC stages. A.**

1404 Immunofluorescence using MAb α -tubulin 12G10 (green) and TgCentrin1 (red) polyclonal
1405 antibody. Centrin staining is not observed in interphase (G1) while diffuse and weak during cell
1406 division (cyt.). **B.** Immunofluorescence using MAb α -tubulin 12G10 (green) and microtubule
1407 (+)-end binding protein TgEB1 polyclonal antibody (red) demonstrates that the cortical
1408 microtubules are relatively short and do not reach the nucleus. **C.** Immunofluorescence using
1409 polyclonal guinea pig BbIMC1a antiserum (see Fig S1 for validation) and MAb α -tubulin 12G10
1410 shows the IMC is present during G/M, outlines budding daughters (cyt.), and extends along the
1411 length of the mature G1 parasites. * marks a recently invaded parasites wherein the cytoskeleton
1412 is completing disassembly; we observed many trophozoites without detectable PbIMC1a. **D.**
1413 Transmission electron microscopy of progressive iRBC developmental stages (1→6). Panel 1 is
1414 a disassembling merozoite already escaped from the vacuole displaying typical pattern of 6
1415 numbered remnants of the disassembling mother IMC. Panel 2 represents early daughter
1416 formation ('Mickey Mouse') with the nucleus being separated into the daughter buds. Panels 3,
1417 4, and 5 represent different sections through developing daughters where showing parallel
1418 assembly (in contrast to polar assembly) consistent with the angle under which the daughter buds
1419 assemble. Panel 6 displays two just divided daughters under the typical angle. N, nucleus, SB
1420 spherical body. Yellow marks IMC; orange arrows mark the typical angle and direction of
1421 daughter buds. Scale bars represent 500 nm. **E.** *Babesia divergens* basal complex upon
1422 completion of cell division. Scale bar represents 500 nm **F.** Schematic of apicomplexan asexual
1423 cell division by binary fission, which mechanistically represents a binary form of schizogony.
1424 Note that the mother's cytoskeleton is largely disassembled following successful host cell
1425 invasion resulting in a pleomorphic cell (2), but that fragments of the IMC are remaining
1426 throughout the division stages (2-4).

Comparative apicomplexan cell division

1427 **Figure 4. Apicomplexan asexual cell division by endodyogeny.** A-E show progressive steps of
1428 cell division as observed for *T. gondii* tachyzoites. Two daughters bud internally, while the
1429 mother's cytoskeleton is maintained and only destabilized just before emergence of nearly
1430 mature daughters (E). A dark blue SFA fiber anchors the centrosomes in the apex of the daughter
1431 buds.

1432
1433 **Figure 5. Endopolygeny with karyokinesis during merogony of *Cystoisospora suis*.** A-D.
1434 Parasites at different stages of endopolygeny. Acetylated (Ac) α -tubulin (red) marks the mother
1435 cells conoid (arrow heads in A, B), subpellicular microtubules, the spindle poles associated with
1436 nuclei undergoing mitosis, and the daughter conoids and subpellicular microtubules (C, D).
1437 Antiserum generated against TgNuf2 (green) marks the clustered kinetochores at mitotic
1438 spindles. A. Eight parasites at different stages in the division cycle. Green numbers indicate the
1439 number of spindle poles seen per mother cell, which is expanding non-geometrically in five of
1440 the parasites indicating asynchronous nuclear cycles. **B.** Five parasites at different stages of
1441 endopolygeny are shown. The parasite on the bottom has five nuclei: nuclei marked "M" are in
1442 early stages of mitosis as 2 spindle poles flanking a single 2N kinetochore cluster are seen; the
1443 circled nuclei represent just completed mitosis as the kinetochore clusters are relatively weak
1444 intensity (1N vs. 2N) and associated with only a single spindle pole. **C, D.** Two examples of cells
1445 at the synchronous daughter budding stage, which both produce 12 daughters as enumerated by
1446 the number of kinetochore clusters, again, consistent with non-geometric expansion of the nuclei.
1447 **E.** Schematic of apicomplexan asexual cell division by endopolygeny with karyokinesis. Note
1448 that the mitotic cycles of the nuclei in the same cytoplasm are not synchronous (2) resulting in
1449 non-geometrically expanded daughter numbers (4-5). Also note that the mother's cytoskeleton is
1450 maintained throughout the meront (technically 'schizont') stages and is only destabilized just
1451 before emergence of nearly mature daughters (5).

1452
1453 **Figure 6. Endopolygeny without nuclear fission by *Sarcocystis neurona* in the intermediate**
1454 **host.** A. Staining of progressive cell division cycle stages (1-4) with α -tubulin (green) marking
1455 the subpellicular microtubules of the mother cytoskeleton (arrow heads), the mitotic spindles (2b,
1456 right parasite; 3) and daughter merozoites subpellicular microtubules (4). Centrin staining (red)
1457 marks the centrosomes, which due to z-stack selection are not visible for all spindles/parasites.

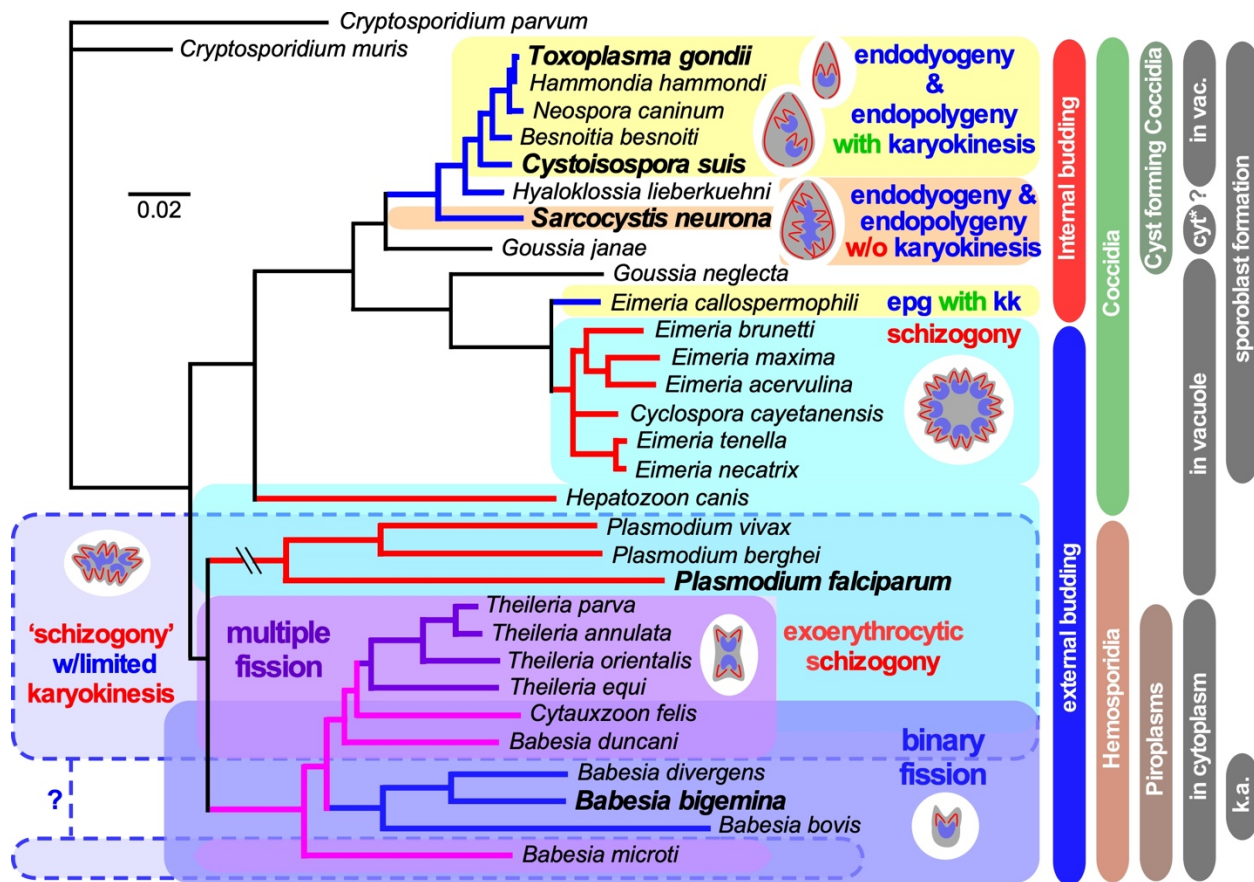
Comparative apicomplexan cell division

1458 Scale bar applies across panels. **B.** Overexpression of a *Toxoplasma* YFP-IMC15 fusion protein
1459 (green) highlights the mother cell's cortical IMC sutures in both panels, whereas in further
1460 progressed panel 2 the bright internal spots mark the centrosomes poised for budding.
1461 Arrowhead marks the apical end of the mother parasite. Panel B modified from (Dubey et al.,
1462 2017). Scale bar applies across panels. **C.** Schematic of apicomplexan asexual cell division by
1463 endopolygeny without karyokinesis. Note the polyploid nuclei undergoing synchronized cycles
1464 of M-phase and mitosis resulting in geometrically expanded daughter cell numbers. Also note
1465 that the mother's cytoskeleton is maintained throughout the schizont stages (2-4) and is only
1466 destabilized just before emergence of nearly mature daughters (5).
1467

Comparative apicomplexan cell division

1468 **Figure 1**

1469

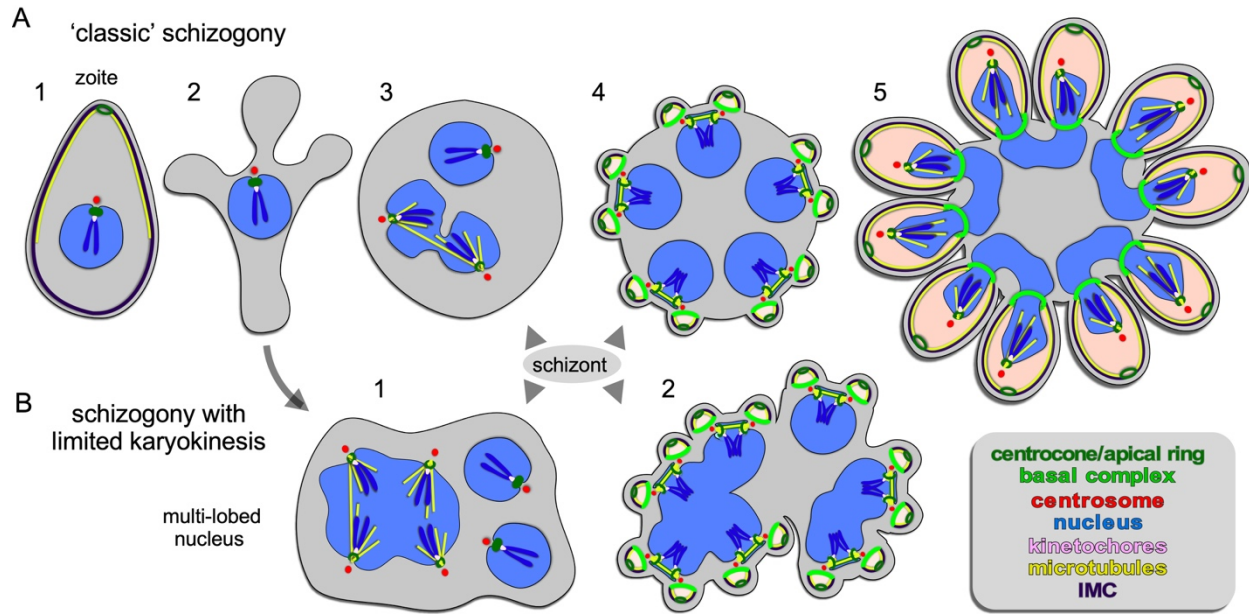


1470

Comparative apicomplexan cell division

1471 **Figure 2**

1472

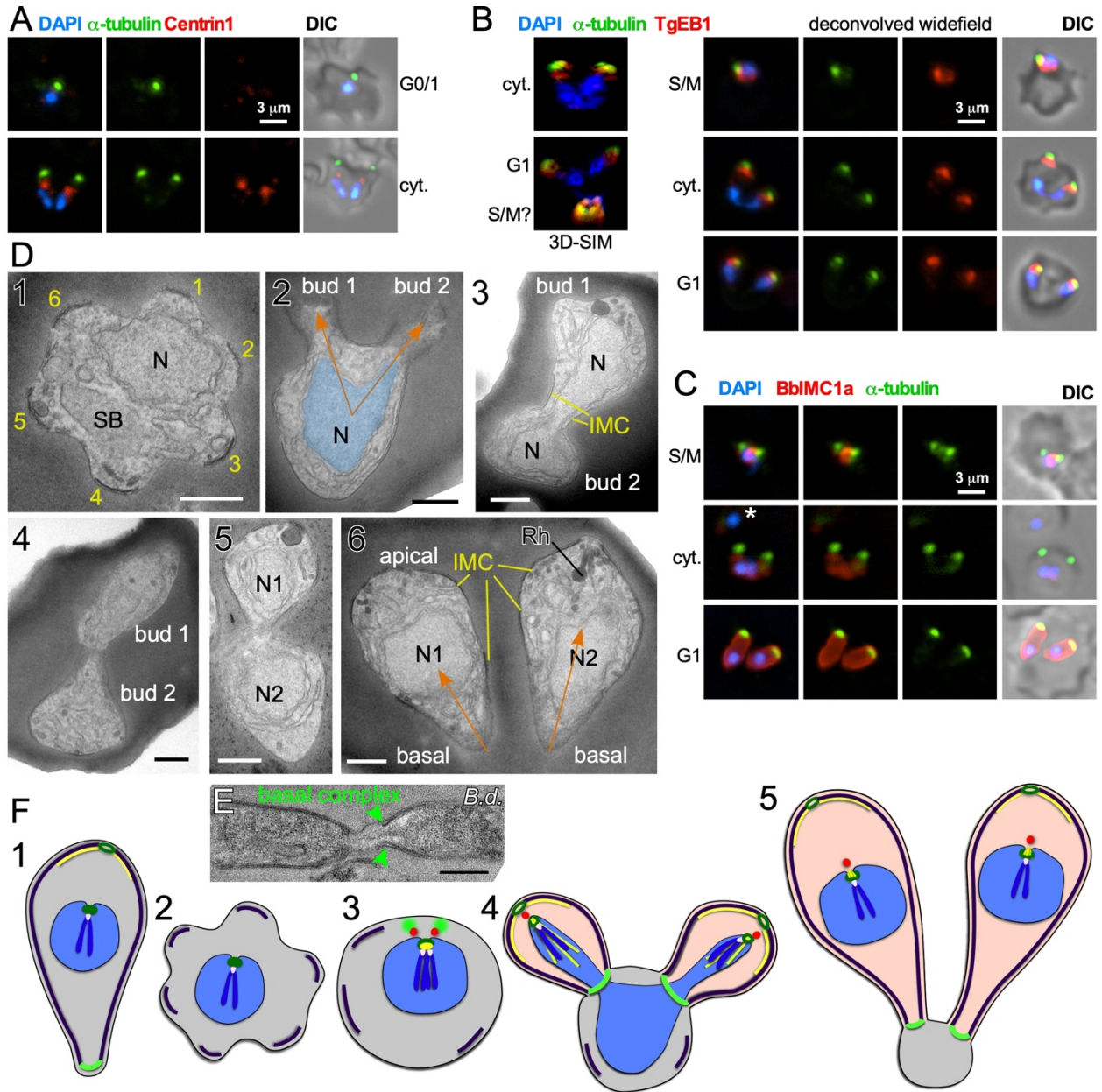


1473

Comparative apicomplexan cell division

1474 **Figure 3**

1475

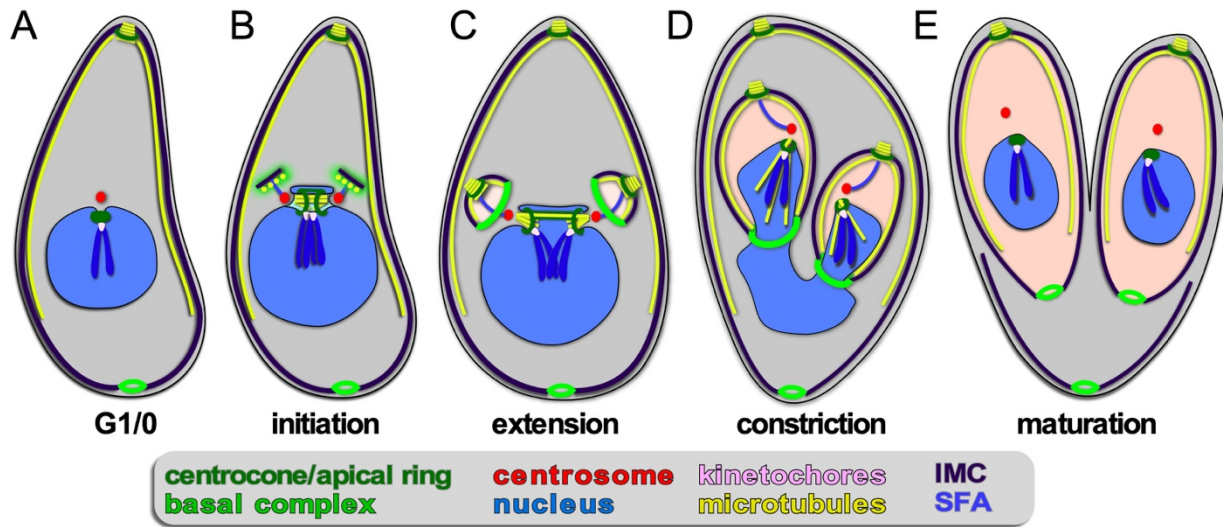


1476

Comparative apicomplexan cell division

1477 **Figure 4**

1478

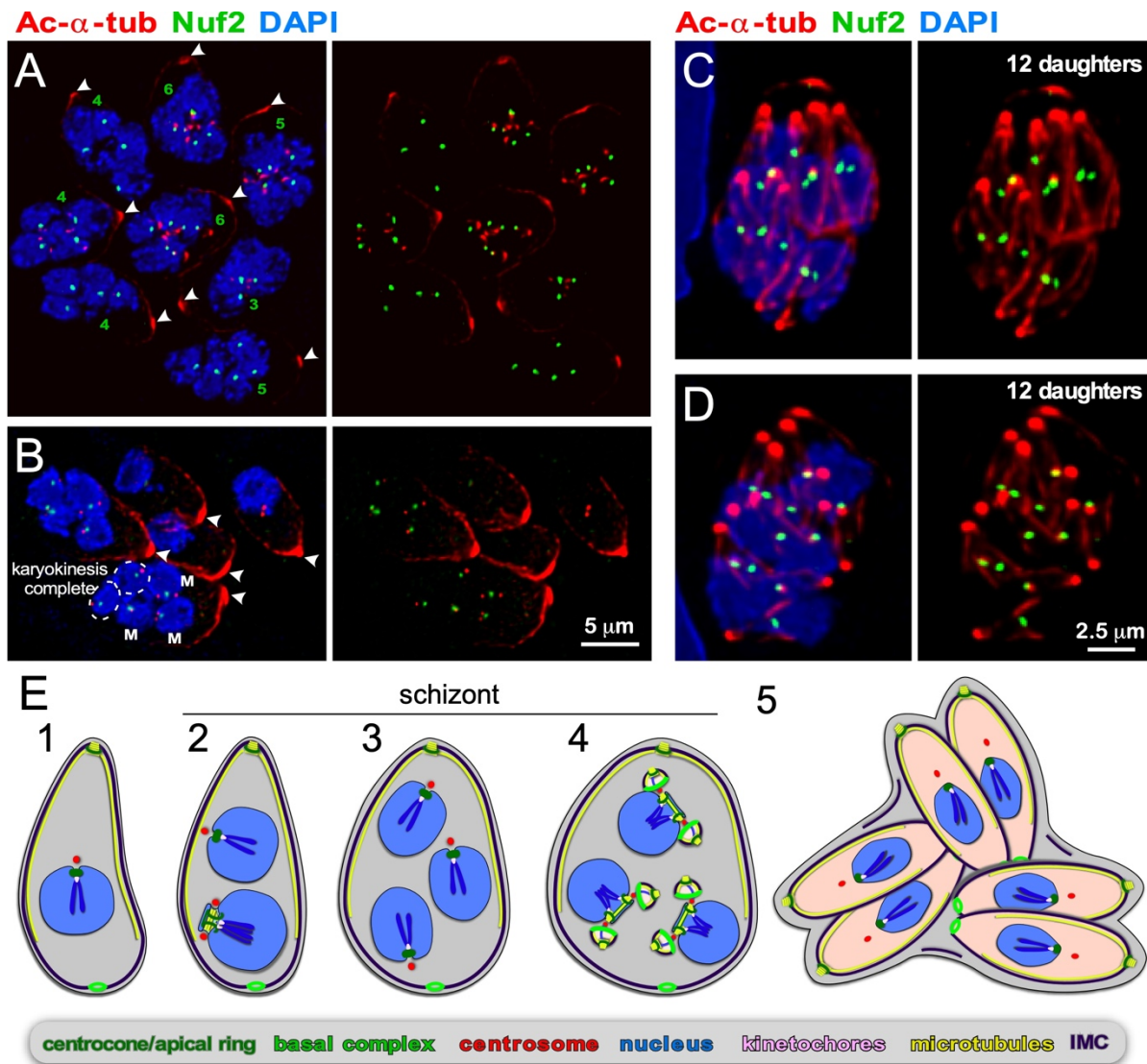


1479

Comparative apicomplexan cell division

1480 **Figure 5**

1481

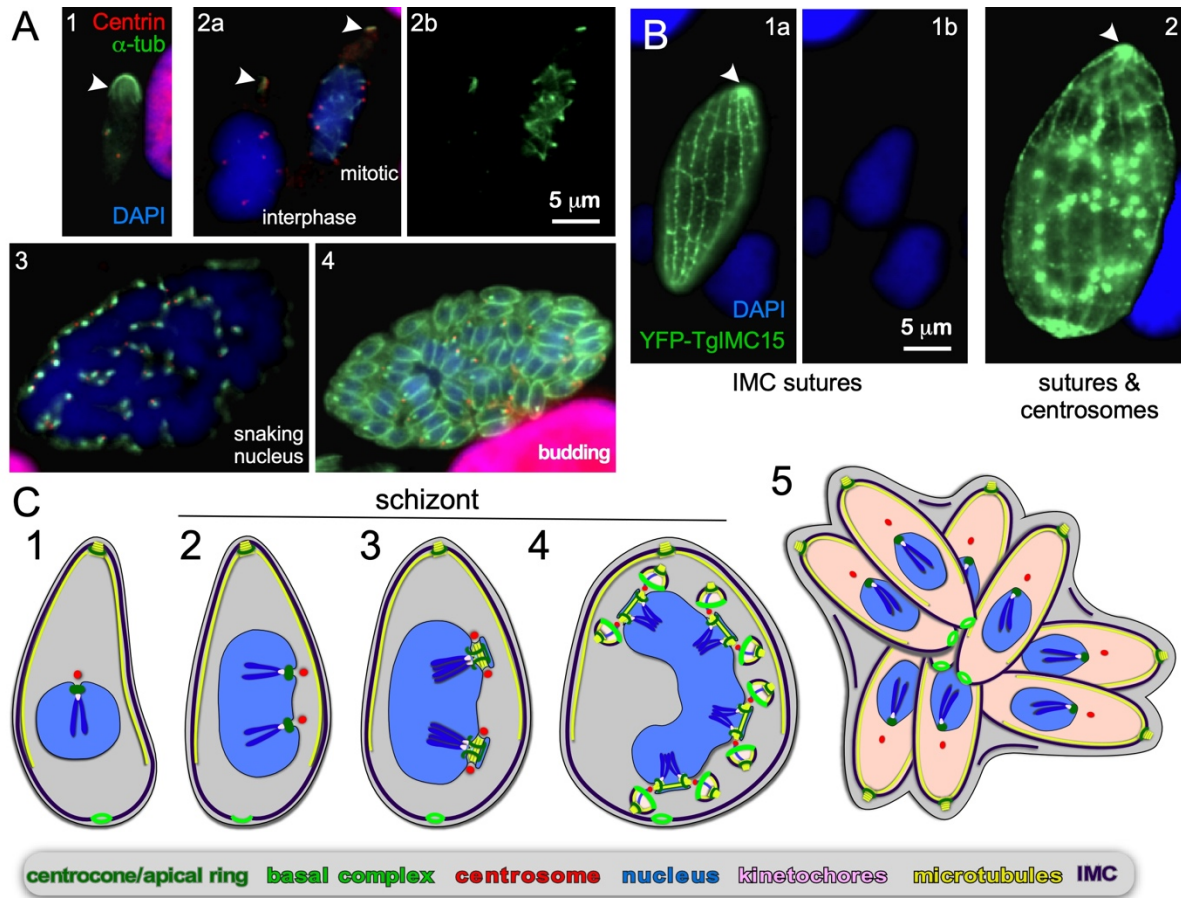


1482

Comparative apicomplexan cell division

1483 **Figure 6**

1484



1485

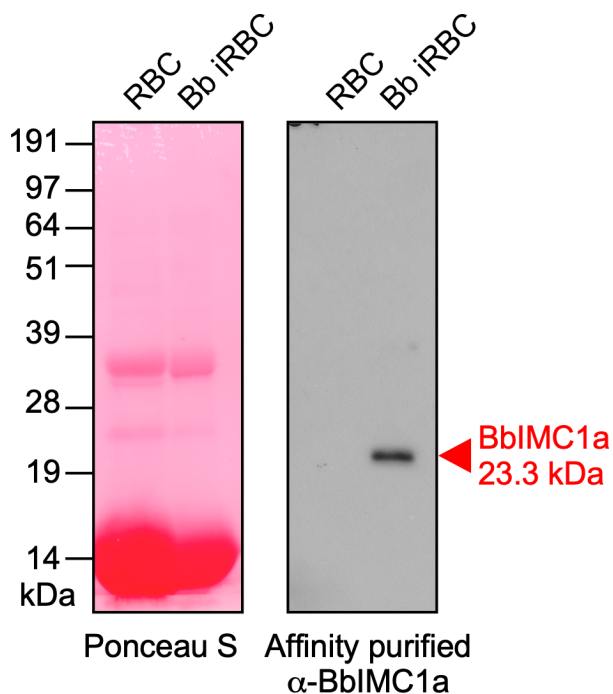
Comparative apicomplexan cell division

1486 **Supplementary Material**

1487

1488 **Figure S1**

1489



1490

1491

1492 **Figure S1. Validation of affinity purified guinea pig antiserum raised against recombinant**

1493 **His6-BbIMC1a by western blot.** Left panel: PonceauS staining of the western blot serving as

1494 loading control; Right panel: serum affinity purified against recombinant His6-BbIMC1a diluted

1495 1:250. RBC indicates cow red blood cell total lysate; Bb iRBC indicates total lysate of cow red

1496 blood cells with a *B. bigemina* parasitemia of 12%. Equal amounts of lysate were loaded across

1497 lanes. The predicted MW of BbIMC1a is 23.3 kDa.